Fermionic massive modes along cosmic strings

Christophe Ringeval

Fermionic massive modes along cosmic strings

Christophe Ringeval
Institut d'Astrophysique de Paris, 98bis boulevard Arago, 75014 Paris, France
(Received 15 June 2001; published 5 November 2001)

The influence on the cosmic string dynamics of fermionic massive bound states propagating in the vortex, and getting their mass only from coupling to the string-forming Higgs field, is studied. Such massive fermionic currents are numerically found to exist for a wide range of model parameters and seen to modify drastically the usual string dynamics coming from the zero mode currents alone. In particular, by means of a quantization procedure, a new equation of state describing cosmic strings with any kind of fermionic current, massive or massless, is derived and found to involve, at least, one state parameter per trapped fermion species. This equation of state exhibits transitions from subsonic to supersonic regimes while the massive modes are filled.

DOI: 10.1103/PhysRevD.64.123505 PACS number(s): 98.80.Cq, 11.27.+d

I. INTRODUCTION

Since it was realized that some early universe phase transitions might lead to the formation of topological defects [1], cosmic strings have been the subject of intense work within the context of cosmology [2]. The large scale structure generated by an ordinary string network in an expanding universe, as well as its imprint on the microwave background, have thus been derived [3,4] in order to state on their significance in the wide range of mechanisms in which they had been originally involved [5,6]. These predictions, compared with the observations, therefore constrain the symmetry breaking schemes effectively realized in the early Universe. These, associated with the most recent data for the microwave background anisotropies [7], even seem to show that such ordinary string networks could not have played the dominant role in the Universe evolution, thereby all the more so constraining the particle physics symmetries leading to their formation. However, as was recently shown [4], a nonnegligible fraction of such defects could have contributed to the overall cosmic microwave background (CMB) anisotropies.

Meanwhile, it was shown by Witten [8] that in realistic physical models, involving various couplings of the string forming Higgs field to other scalar or fermion fields, currents could build along the strings, turning them into ''superconducting wires.'' Without even introducing couplings with the electromagnetic fields [9], the breaking of Lorentz invariance along the vortex induced by such currents may drastically modify the string properties, and thus the cosmological evolution of the associated networks. In particular, cosmic string loops can reach centrifugally supported equilibrium state, called vortons [10], that would completely dominate the Universe [11]. Theories predicting stable vortons thus turn out to be incompatible with observational cosmology, hence the particular interest focused on ''superconducting'' models.

Unfortunately, all the new properties and cosmological consequences stemming from string conductivity have not yet been clearly established, because of the complicated, and somehow arbitrary, microphysics possible in these models. However, although the microscopic properties induced by such currents depend on the explicit underlying field theory [12,13], a macroscopic formalism was introduced by Carter [14] which permits a unified description of the string dynamics through the knowledge of its energy per unit length U and tension T. These end up being functions of a so-called state parameter w, as the current itself, through an equation of state. Such a formalism is, in particular, well designed for scalar currents, as shown in, e.g., Refs. [15,16]: due to their bosonic nature, all trapped scalar particles go into the lowest accessible state, and thus can be described through the classical values taken by the relevant scalar fields [17]. The induced gravitational field [18,19] or the back reaction effects [20] depend only on this state parameter. The classical string stability [21,22] has already been investigated for various equations of state relating U and T, on the basis of scalar and chiral currents microphysics [23,24]. Moreover, it was also shown, through a semiclassical approach, that fermionic current carrying cosmic strings, even though in principle involving more than one state parameter [25], can also be described by an equation of state of the so-called ''fixed trace'' kind, i.e., $U+T=2M^2$. Such a relationship has the property of allowing stable loop configurations to exist, at least at the classical level [22]. Nevertheless, these results have been derived for fermionic currents flowing along the string in the form of zero modes only, as they were originally introduced by Witten [8], although it was shown that the fermions may also be trapped in the vortex with nonvanishing masses [26]; hence the following work in which the influence of such massive modes is studied for the simplest of all fermionic Witten model.

In this paper, after deriving numerically the relevant properties of the trapped massive wave solutions of the Dirac equation in the vortex, we show that the quantization procedure, originally performed to deal with the fermionic zero modes [25], can be generalized to include the massive ones, and leads to a new equation of state with more than one state parameter. In particular, it is found that the fixed trace equation of state, that holds for massless fermionic currents alone, is no longer verified. Besides, the massive modes are actually found to rapidly dominate the string dynamics, thereby modifying the classical vorton stability induced by the zero modes alone.

Let us sketch the lines along which this work is made. In

Sec. II, the model and the notations are set, while we derive the equations of motion. Then, in Sec. III, by means of a separation between transverse and longitudinal degrees of freedom of the spinor fields, the massive wave solutions along the string are computed numerically for a wide range of fermion charges and coupling constants. The constraint of transverse normalizability is found to be satisfied only for particular values of the trapped modes mass, $\bar{m}$ say, whose dependence with the model parameters is investigated. The two-dimensional quantization of the $\bar{m}$ normalizable massive modes is then performed in Sec. IV, using the canonical procedure. In the way previously discussed in the case of zero modes [25], the conserved quantities, i.e., energy-momentum tensor and charge currents, are then expressed in their quantum form. Their average values, in the zero-temperature case, and infinite string limit, lead to macroscopic expressions for the energy per unit length U and tension T, which end up being functions of the number densities of fermions propagating along the string. Their derivation and extension to any kind and number of fermionic carriers is performed in Sec. V, while the cosmological consequences of this new analysis are briefly discussed in the concluding section.

II. MODEL

We shall consider here an Abelian Higgs model with scalar Φ and gauge field B_μ, coupled, following Witten [8], to two spinor fields, Ψ and $\mathcal{X}$ say. Since we are only interested in the purely dynamical effects the current may induce on the strings, we will not consider any additional electromagnetic-like coupling of the fermion fields to an extra gauge field. Thus we consider here the so-called ''neutral limit'' [15].

A. Microscopic Lagrangian

The previous assumptions imply one needs one local $U(1)$ symmetry which is spontaneously broken through the Higgs mechanism, yielding vortices formation. The Higgs field is chosen as complex scalar field with conserved charge qc_ϕ under the local $U(1)$ symmetry, associated with a gauge vector field B_μ. The two spinor fields acquire masses from a chiral coupling to the Higgs field, and have opposite electromagnetic charges in order for the full (four-dimensional) model to be anomaly free [8]. Under the broken symmetry they also have conserved charges $qc_{\psi_{\rm R}}$, $qc_{\psi_{\rm L}}$ and $qc_{\chi_{\rm R}}$, $qc_{\chi_{\rm L}}$ for their right- and left-handed parts, respectively. With $\mathcal{L}_{\rm h}$, $\mathcal{L}_{\rm g}$ and $\mathcal{L}_\psi$, $\mathcal{L}_\chi$, the Lagrangian in the Higgs, gauge, and fermionic sectors, respectively, the theory reads

$$\mathcal{L}=\mathcal{L}_{\rm h}+\mathcal{L}_{\rm g}+\mathcal{L}_\psi+\mathcal{L}_\chi, \tag{1}$$

with

$$\mathcal{L}_{\rm h}=\frac{1}{2}(D_\mu\Phi)^\dagger(D^\mu\Phi)-V(\Phi), \tag{2}$$

$$\mathcal{L}_{\rm g}=-\frac{1}{4}H_{\mu\nu}H^{\mu\nu}, \tag{3}$$

$$\mathcal{L}_\psi=\frac{i}{2}[\bar{\Psi}\gamma^\mu D_\mu\Psi-(\overline{D_\mu\Psi})\gamma^\mu\Psi] -g\bar{\Psi}\frac{1+\gamma_5}{2}\Psi\Phi-g\bar{\Psi}\frac{1-\gamma_5}{2}\Psi\Phi^*, \tag{4}$$

$$\mathcal{L}_\chi=\frac{i}{2}[\bar{\mathcal{X}}\gamma^\mu D_\mu\mathcal{X}-(\overline{D_\mu\mathcal{X}})\gamma^\mu\mathcal{X}] -g\bar{\mathcal{X}}\frac{1+\gamma_5}{2}\mathcal{X}\Phi^*-g\bar{\mathcal{X}}\frac{1-\gamma_5}{2}\mathcal{X}\Phi, \tag{5}$$

where the $U(1)$ field strength tensor and the scalar potential are

$$H_{\mu\nu}=\nabla_\mu B_\nu-\nabla_\nu B_\mu, \tag{6}$$

$$V(\Phi)=\frac{\lambda}{8}(|\Phi|^2-\eta^2)^2, \tag{7}$$

while covariant derivatives involve the field charges through

$$D_\mu\Phi=(\nabla_\mu+iqc_\phi B_\mu)\Phi, \tag{8}$$

$$D_\mu\Psi=\left(\nabla_\mu+iq\frac{c_{\psi_{\rm R}}+c_{\psi_{\rm L}}}{2}B_\mu +iq\frac{c_{\psi_{\rm R}}-c_{\psi_{\rm L}}}{2}\gamma_5 B_\mu\right)\Psi, \tag{9}$$

$$D_\mu\mathcal{X}=\left(\nabla_\mu+iq\frac{c_{\chi_{\rm R}}+c_{\chi_{\rm L}}}{2}B_\mu +iq\frac{c_{\chi_{\rm R}}-c_{\chi_{\rm L}}}{2}\gamma_5 B_\mu\right)\mathcal{X}, \tag{10}$$

and the relation

$$c_{\psi_{\rm L}}-c_{\psi_{\rm R}}=c_\phi=c_{\chi_{\rm R}}-c_{\chi_{\rm L}} \tag{11}$$

should hold in order for the Yukawa terms in $\mathcal{L}_\psi$ and $\mathcal{L}_\chi$ to be gauge invariant.

B. Basic equations

This theory admits vortex solutions which are expected to form in the early Universe by means of the Kibble mechanism [1]. A cosmic string configuration can be chosen to lie along the z axis, and we will use Nielsen-Olesen solutions of the field equations [27]. In cylindrical coordinates, the string forming Higgs and gauge fields thus read

$$\Phi=\varphi(r)e^{in\theta}, \quad B_\mu=B(r)\,\delta_{\mu\theta}, \tag{12}$$

where the winding number n is an integer, in order for the Higgs field to be single valued under rotation around the string. In such vortex background, the equations of motion in the fermionic sector, for both spinor fields $\mathcal{F}$ read (here and

in various places throughout this paper, we shall denote by $\mathcal{F}$ an arbitrary fermion, namely a spinor Ψ or $\mathcal{X}$)

$$i\gamma^{\mu}\nabla_{\mu}\mathcal{F}=\frac{\partial j^{\mu}_{\mathcal{F}}}{\partial\bar{\mathcal{F}}}B_{\mu}+M_{\mathcal{F}}\mathcal{F} \tag{13}$$

with the fermionic gauge currents

$$j^{\mu}_{\mathcal{F}}=q\frac{c_{\mathcal{F}_{\mathrm{R}}}+c_{\mathcal{F}_{\mathrm{L}}}}{2}\bar{\mathcal{F}}\gamma^{\mu}\mathcal{F}+q\frac{c_{\mathcal{F}_{\mathrm{R}}}-c_{\mathcal{F}_{\mathrm{L}}}}{2}\bar{\mathcal{F}}\gamma^{\mu}\gamma_5\mathcal{F}, \tag{14}$$

and the mass terms

$$M_{\psi}=g\varphi\cos n\theta+ig\varphi\gamma_5\sin n\theta, \tag{15}$$

$$M_{\chi}=g\varphi\cos n\theta-ig\varphi\gamma_5\sin n\theta. \tag{16}$$

Note the fermionic currents have an axial and vectorial component because of the chiral coupling of the fermions to the Higgs field, as can be seen through the mass terms $M_{\mathcal{F}}$ in Eqs. (15) and (16). Moreover, since the Higgs field vanishes in the string core while taking nonzero vacuum expectation value, η say, outside, the mass term acts as an attractive potential. As a result, fermionic bound states, with energy between zero and $g\eta$, are expected to exist and propagate in the string core.

III. FERMIONIC BOUND STATES

A. Trapped wave solutions

Since the string is assumed axially symmetric, it is convenient to look for trapped solutions of the fermionic equations of motion, by separating longitudinal and transverse dependencies of the spinor fields. Using the same notations as in Ref. [25], the two-dimensional plane-wave solutions along the string, for both fermions, read

$$\Psi^{(\varepsilon)}_{\mathrm{p}}=\mathrm{e}^{\varepsilon i(\omega t-kz)}\begin{pmatrix}\xi_1(r)\mathrm{e}^{-im_1\theta}\\ \xi_2(r)\mathrm{e}^{-im_2\theta}\\ \xi_3(r)\mathrm{e}^{-im_3\theta}\\ \xi_4(r)\mathrm{e}^{-im_4\theta}\end{pmatrix},$$

$$\mathcal{X}^{(\varepsilon)}_{\mathrm{p}}=\mathrm{e}^{\varepsilon i(\omega t-kz)}\begin{pmatrix}\zeta_1(r)\mathrm{e}^{-il_1\theta}\\ \zeta_2(r)\mathrm{e}^{-il_2\theta}\\ \zeta_3(r)\mathrm{e}^{-il_3\theta}\\ \zeta_4(r)\mathrm{e}^{-il_4\theta}\end{pmatrix}, \tag{17}$$

where $\varepsilon=\pm1$ labels the positive and negative energy solutions. Similarly to the Higgs field case, the winding numbers of the fermions, m_i and l_i, are necessary integers. In order to simplify the notations, it is more convenient to work with dimensionless scaled fields and coordinates. With $m_{\mathrm{h}}=\eta\sqrt{\lambda}$ the mass of the Higgs boson, we can write

$$\varphi=\eta H,\quad Q=n+qc_{\phi}B,\quad \text{and}\quad r=\frac{\varrho}{m_{\mathrm{h}}}. \tag{18}$$

In the same way, the spinorial components of the Ψ field are rescaled as

$$\xi_1(\varrho)=\frac{m_{\mathrm{h}}}{\sqrt{2\pi}}\sqrt{\omega+k}\,\tilde{\alpha}_1(\varrho),\quad \xi_2(\varrho)=i\frac{m_{\mathrm{h}}}{\sqrt{2\pi}}\sqrt{\omega-k}\,\tilde{\alpha}_2(\varrho),$$

$$\xi_3(\varrho)=\frac{m_{\mathrm{h}}}{\sqrt{2\pi}}\sqrt{\omega-k}\,\tilde{\alpha}_3(\varrho),\quad \xi_4(\varrho)=i\frac{m_{\mathrm{h}}}{\sqrt{2\pi}}\sqrt{\omega+k}\,\tilde{\alpha}_4(\varrho). \tag{19}$$

In the chiral representation, and with the metric signature $(+,-,-,-)$, in terms of these new variables, Eqs. (13) and (17) yield, for the Ψ field,

$$\mathrm{e}^{-i(m_1-1)\theta}\left[\frac{\mathrm{d}\tilde{\alpha}_1}{\mathrm{d}\varrho}-\tilde{f}_1(\varrho)\tilde{\alpha}_1(\varrho)\right]=\varepsilon\frac{\bar{m}}{m_{\mathrm{h}}}\mathrm{e}^{-im_2\theta}\tilde{\alpha}_2(\varrho)-\frac{m_{\mathrm{f}}}{m_{\mathrm{h}}}H(\varrho)\mathrm{e}^{-i(m_4+n)\theta}\tilde{\alpha}_4(\varrho),$$

$$\mathrm{e}^{-i(m_2+1)\theta}\left[\frac{\mathrm{d}\tilde{\alpha}_2}{\mathrm{d}\varrho}-\tilde{f}_2(\varrho)\tilde{\alpha}_2(\varrho)\right]=-\varepsilon\frac{\bar{m}}{m_{\mathrm{h}}}\mathrm{e}^{-im_1\theta}\tilde{\alpha}_1(\varrho)+\frac{m_{\mathrm{f}}}{m_{\mathrm{h}}}H(\varrho)\mathrm{e}^{-i(m_3+n)\theta}\tilde{\alpha}_3(\varrho),$$

$$\mathrm{e}^{-i(m_3-1)\theta}\left[\frac{\mathrm{d}\tilde{\alpha}_3}{\mathrm{d}\varrho}-\tilde{f}_3(\varrho)\tilde{\alpha}_3(\varrho)\right]=-\varepsilon\frac{\bar{m}}{m_{\mathrm{h}}}\mathrm{e}^{-im_4\theta}\tilde{\alpha}_4(\varrho)+\frac{m_{\mathrm{f}}}{m_{\mathrm{h}}}H(\varrho)\mathrm{e}^{-i(m_2-n)\theta}\tilde{\alpha}_2(\varrho),$$

$$\mathrm{e}^{-i(m_4+1)\theta}\left[\frac{\mathrm{d}\tilde{\alpha}_4}{\mathrm{d}\varrho}-\tilde{f}_4(\varrho)\tilde{\alpha}_4(\varrho)\right]=\varepsilon\frac{\bar{m}}{m_{\mathrm{h}}}\mathrm{e}^{-im_3\theta}\tilde{\alpha}_3(\varrho)-\frac{m_{\mathrm{f}}}{m_{\mathrm{h}}}H(\varrho)\mathrm{e}^{-i(m_1-n)\theta}\tilde{\alpha}_1(\varrho), \tag{20}$$

where $m_{\mathrm{f}}=g\eta$ is the fermion mass in the vacuum in which the Higgs field takes its vacuum expectation value η, and $\bar{m}=\sqrt{\omega^2-k^2}$ is the mass of the trapped mode. The coupling to the gauge field B_{μ} appears through the purely radial functions $\tilde{f}$:

$$\tilde{f}_1(\varrho)=\frac{c_{\psi_{\mathrm{R}}}}{c_{\phi}}\frac{Q-n}{\varrho}-\frac{m_1}{\varrho},\quad \tilde{f}_2(\varrho)=-\frac{c_{\psi_{\mathrm{R}}}}{c_{\phi}}\frac{Q-n}{\varrho}+\frac{m_2}{\varrho},$$

$$\tilde{f}_3(\varrho)=\frac{c_{\psi_{\mathrm{L}}}}{c_{\phi}}\frac{Q-n}{\varrho}-\frac{m_3}{\varrho},\quad \tilde{f}_4(\varrho)=-\frac{c_{\psi_{\mathrm{L}}}}{c_{\phi}}\frac{Q-n}{\varrho}+\frac{m_4}{\varrho}. \tag{21}$$

The spinor field $\mathcal{X}$ verifies the same equations apart from the fact that, due to its coupling to $\Phi^{\dagger}$ [see Eq. (5)], it is necessary to transform $n\rightarrow-n$.

As was originally found by Jackiw and Rossi [28] and Witten [8], there are always n normalizable zero energy solutions of the Dirac operator in the vortex which allow fermions to propagate at the speed of light in the "$-z$" and "$+z$," say, directions, for the Ψ and $\mathcal{X}$ fields, respectively. These solutions are found to be eigenvectors of the $\gamma^0\gamma^3$ operator and are clearly obtained from the above equations by setting the consistency angular relationships $m_1-1=m_4+n$ and $m_2+1=m_3+n$, those leading to the zero mode dispersion relation $\bar{m}=0\Leftrightarrow\omega=\pm k$. Note that only one eigenstate of $\gamma^0\gamma^3$ end up being normalizable for each kind of chiral coupling to the Higgs field, and thus the relevant dispersion relations reduce to $\omega=-k$ and $\omega=k$, for the Ψ and $\mathcal{X}$ zero modes, respectively [25].

Such zero modes have a simple interpretation: since the Higgs field vanishes in the string core, the mass term $M_{\mathcal{F}}$ in Eq. (13) vanishes too, and the fermions trapped in have zero mass. As a result, they propagate at the speed of light and they verify the dispersion relations $\omega=k$ or $\omega=-k$.

B. Massive trapped waves

However, it is also possible *a priori*, for the trapped fermions, to explore outer regions surrounding the string core where the Higgs field takes nonexactly vanishing values. In practice, this is achieved by means of a nonvanishing fermion angular momentum, which will lead to a nonvanishing effective mass $\bar{m}^2=\omega^2-k^2\neq 0$. For the Ψ field, such massive solutions of the equations of motion (20) can only be obtained for four-dimensional solutions, in order to ease the zero mode constraint $\omega=\pm k$. The required angular consistency relations therefore read

$$m=m_1=m_2+1=m_3+n=m_4+n+1. \tag{22}$$

Similarly, the angular dependence of $\mathcal{X}$ field has to verify analogous conditions with the transformation $n\rightarrow -n$. It was previously shown numerically that the Abelian Higgs model with one Weyl spinor always admits such kind of normalizable solutions [26]. In the following, massive solutions for Dirac spinors are numerically derived for our model and shown to exist for a wide range of fermion charges and coupling constants.

1. Analytical considerations

Some interesting analytical asymptotic behaviors of these modes have been previously studied [25,26]. In particular, there are only two degenerate *normalizable* eigensolutions of Eqs. (20) at infinity. Since the Higgs field goes to its constant vacuum expectation value and the gauge coupling functions vanish, we found the eigensolutions to scale as $\exp(\pm\Omega\varrho)$, with

$$\Omega=\sqrt{\frac{m_{\mathrm{f}}^2-\bar{m}^2}{m_{\mathrm{h}}^2}}. \tag{23}$$

First, note that in order to have decreasing solutions at infinity, the mass of the trapped modes $\bar{m}$ has to be less than the fermion vacuum mass m_{f}, as intuitively expected (for $\bar{m}>m_{\mathrm{f}}$, one recovers the oscillating behavior that is typical of free particle solutions). Moreover, from Cauchy theorem, two degrees of freedom can be set in order to keep only the two well defined solution at infinity. On the other hand, by looking at the power-law expansion of both system and solutions near the string core [25,28], only two such solutions are also found to be normalizable. More precisely, normalizability of each eigensolution at $\varrho=0$ leads to one condition on the winding numbers m_i of each spinorial component ξ_i. Moreover, in order for the fermion field to be well defined by rotation around the string, each spinorial component ξ_i with nonzero winding number m_i has to vanish in the string core, and so behaves like a positive power of the radial distance to the core. The analytical expression of the eigensolutions near $\varrho=0$ reads [25]

$$\begin{pmatrix}\xi_1\\ \xi_2\\ \xi_3\\ \xi_4\end{pmatrix}_{s_1}\sim\begin{pmatrix}a_1\varrho^{-m}\\ a_2(a_1)\varrho^{-m+1}\\ a_3(a_1)\varrho^{-m+|n|+2}\\ a_4(a_1)\varrho^{-m+|n|+1}\end{pmatrix},$$

$$\begin{pmatrix}\xi_1\\ \xi_2\\ \xi_3\\ \xi_4\end{pmatrix}_{s_2}\sim\begin{pmatrix}a_1\varrho^{m+|n|-n}\\ a_2(a_1)\varrho^{m+|n|-n+1}\\ a_3(a_1)\varrho^{m-n}\\ a_4(a_1)\varrho^{m-n-1}\end{pmatrix},$$

$$\begin{pmatrix}\xi_1\\ \xi_2\\ \xi_3\\ \xi_4\end{pmatrix}_{s_3}\sim\begin{pmatrix}a_1\varrho^{m}\\ a_2(a_1)\varrho^{m-1}\\ a_3(a_1)\varrho^{m+|n|}\\ a_4(a_1)\varrho^{m+|n|+1}\end{pmatrix},$$

$$\begin{pmatrix}\xi_1\\ \xi_2\\ \xi_3\\ \xi_4\end{pmatrix}_{s_4}\sim\begin{pmatrix}a_1\varrho^{-m+|n|+n+2}\\ a_2(a_1)\varrho^{-m+|n|+n+1}\\ a_3(a_1)\varrho^{-m+n}\\ a_4(a_1)\varrho^{-m+n+1}\end{pmatrix}. \tag{24}$$

The normalizability condition for the four eigensolutions can be summarized by

$$\sup(0,n)<m<\inf(1,1+n), \tag{25}$$

and so, for any value of m there are only two conditions satisfied. However, from the consistency angular conditions on each spinorial components, only three pairs of solutions are acceptable near the string. Assuming $n>0$, if $m\leqslant 0$ then only the pair (s_1,s_4) is both normalizable and well defined by rotation around the vortex, similarly for $m\geqslant n+1$ the relevant solutions are (s_2,s_3), whereas for $1\leqslant m\leqslant n$, they are (s_3,s_4). As a result, the two remaining degrees of freedom can be set to get only these pairs near the string core for a given value of m, but there is no reason that they should match with the two normalizable solutions at infinity. In or-

der to realize this matching we have to fine tune another parameter which turns out to be the mass of the modes, $\bar{m}$. As expected for bound states, this mass is therefore necessarily quantized. Note at this point that $\bar{m}=0$ is, in such a procedure, nothing but a particular case of the general solution here presented. The three different pairs of well defined solutions at the origin suggest that there are three kinds of similar massive bound states in the vortex, according to the values of the winding number m. Intuitively, the more the field winds around the string, the farther the particle explores regions surrounding the core due to the higher values taken by its angular momentum, meaning the largest the extension of its wave function is, the more it acquires mass from coupling to a nonexactly vanishing Higgs field. As a result, the lowest massive modes will certainly be obtained from values of m which correspond to vanishing winding numbers m_i.

2. Symmetries

In the following, the equations of motion (20) will be summarized in the form $(\mathcal{S}_\varepsilon)_i^j\tilde{\alpha}_j=0$, with implicit summation implied over repeated indices.

The first symmetry is obtained from the complex conjugation of the equations of motion (20). Since complex conjugation does not modify Eqs. (20), once the angular consistency relations (22) are set, there is an arbitrary complex phase in the choice of solutions, and it will be sufficient to look for real rescaled spinorial components $\tilde{\alpha}_i$.

There is another symmetry between the positive and negative energy solutions of the equations of motion (20) that may be useful. With the label $\varepsilon=\pm$ for particle and antiparticle states, respectively, one has

$$(\mathcal{S}_+)_i^j\tilde{\alpha}_{j_+}=0 \quad \Rightarrow \quad (\mathcal{S}_-)_i^j\tilde{\alpha}_{j_-}=0, \tag{26}$$

provided

$$\tilde{\alpha}_{i_-}=(\gamma^0\gamma^3)_i^j\tilde{\alpha}_{j_+}. \tag{27}$$

As a result, the negative energy solutions are obtained from the positive ones by the action of the $\gamma^0\gamma^3$ operator, thereby generalizing the properties of the zero modes which were precisely found as eigenstates of this operator [8,25,28].

The last symmetry concerns the gauge coupling functions $\tilde{f}_i$. Under the transformations

$$\begin{aligned} m&\to\hat{m}=n+1-m,\\ c_{\psi_{\rm L}}&\to\hat{c}_{\psi_{\rm L}}=-c_{\psi_{\rm R}},\\ c_{\psi_{\rm R}}&\to\hat{c}_{\psi_{\rm R}}=-c_{\psi_{\rm L}}, \end{aligned} \tag{28}$$

the gauge functions $\tilde{f}_i$, in Eqs. (20), are simply swapped according to $\tilde{f}_1\leftrightarrow\tilde{f}_4$ and $\tilde{f}_2\leftrightarrow\tilde{f}_3$. As a result, for every $\tilde{\alpha}$ solution found at given $c_{\psi_{\rm L}}$ and m, there is another solution $\hat{\alpha}$, with charge $\hat{c}_{\psi_{\rm L}}=c_\phi-c_{\psi_{\rm L}}$ and winding number $\hat{m}=n+1-m$, namely

$$\begin{aligned} &\hat{\alpha}_1(\varrho)=\tilde{\alpha}_4(\varrho), \quad \hat{\alpha}_2(\varrho)=\tilde{\alpha}_3(\varrho),\\ &\hat{\alpha}_3(\varrho)=\tilde{\alpha}_2(\varrho), \quad \hat{\alpha}_4(\varrho)=\tilde{\alpha}_1(\varrho). \end{aligned} \tag{29}$$

Note that the particular case $c_{\psi_{\rm L}}=\hat{c}_{\psi_{\rm L}}=c_\phi/2$ appears as a frontier separating two symmetric kinds of solutions with two differents winding numbers lying on both sides of $m=(n+1)/2$. As a result, the three different behaviors found above from normalization and angular consistency conditions seem to reduce to only two, since the domains where $m\leqslant 0$ and $m\geqslant n+1$ are actually connected by charge symmetry in relation to $c_\phi/2$.

On the other hand, due to its coupling to the antivortex instead of the vortex, the equations of motion of the $\mathcal{X}$ field are simply obtained from Eqs. (20) by the transformations $\tilde{\alpha}_i\to\tilde{\beta}_j$, $c_{\psi_{\rm L(R)}}\to c_{\chi_{\rm L(R)}}$, and $m_i\to l_i$. The l_i are the winding numbers of the scaled $\mathcal{X}$ spinorial components, namely the $\tilde{\beta}_i$, and they verify the angular consistency relations (22) with n replaced by $-n$ as previously discussed. Let us introduce one more transformation on the Ψ parameters,

$$\begin{aligned} m&\to\hat{m}=l+n,\\ c_{\psi_{\rm L}}&\to\hat{c}_{\psi_{\rm L}}=c_{\chi_{\rm R}},\\ c_{\psi_{\rm R}}&\to\hat{c}_{\psi_{\rm R}}=c_{\chi_{\rm L}}. \end{aligned} \tag{30}$$

Naming $\tilde{g}_i$ the scaled gauge coupling functions of the $\mathcal{X}$ spinor, the Ψ ones are found to transform according to $\tilde{f}_1\to\tilde{g}_3$, $\tilde{f}_2\to\tilde{g}_4$, $\tilde{f}_3\to\tilde{g}_1$, and $\tilde{f}_4\to\tilde{g}_2$. Thus, if the $\tilde{\alpha}$ are solutions of the Ψ equations of motion (20), with m winding number and $c_{\psi_{\rm L}}$ charge, then there exist $\tilde{\beta}$ solutions for the $\mathcal{X}$ field with same mass $\bar{m}$, provided $l=m-n$ and $c_{\chi_{\rm L}}=c_{\psi_{\rm R}}=c_{\psi_{\rm L}}-c_\phi$, and they read

$$\begin{aligned} &\tilde{\beta}_1(\varrho)=\tilde{\alpha}_3(\varrho), \quad \tilde{\beta}_2(\varrho)=-\tilde{\alpha}_4(\varrho),\\ &\tilde{\beta}_3(\varrho)=\tilde{\alpha}_1(\varrho), \quad \tilde{\beta}_4(\varrho)=-\tilde{\alpha}_2(\varrho). \end{aligned} \tag{31}$$

Owing to these symmetries, it is sufficient to study the Ψ equations of motion (20), for various values of the winding number m and for left-handed part charges, namely $c_{\psi_{\rm L}}$, higher or equal than $c_\phi/2$.

3. Numerical methods

In order to compute the relevant massive wave solutions for the Ψ fermions on the string, it is necessary to solve first the vortex background. At zeroth order, neglecting the back reaction of the fermionic currents, and in terms of the dimensionless fields and parameters, the equations of motion for the string forming Higgs and gauge fields read, from Eq. (1),

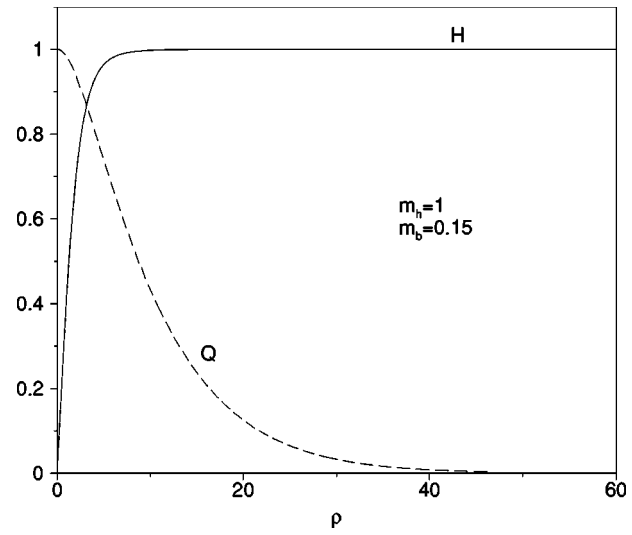

FIG. 1. The solutions of the field equations for the vortex background. The Higgs field H takes its vacuum expectation value at infinity and the gauge bosons condensate in the vortex.

$$\frac{d^2H}{d\varrho^2}+\frac{1}{\varrho}\frac{dH}{d\varrho}=\frac{HQ^2}{\varrho^2}+\frac{1}{2}H(H^2-1), \tag{32}$$

$$\frac{d^2Q}{d\varrho^2}-\frac{1}{\varrho}\frac{dQ}{d\varrho}=\frac{m_b^2}{m_h^2}H^2Q, \tag{33}$$

where $m_b=qc_\phi\eta$ is the classical mass of the gauge boson. The solution of these equations is well known [15,17,29] and shown in Fig. 1 for a specific (assumed generic) set of parameters.

The system of Eqs. (20) being linear and involving only first-order derivatives of the spinor components, a Runge-Kutta numerical method of integration has been used. However, as noted above, since we are interested only in normalizable solutions, it is more convenient to perform the resolution from an arbitrary cutoff at infinity, toward the string core. Let us introduce ϱ_∞, the cutoff value on the dimensionless radial distance. From the asymptotic form of Eqs. (20) at infinity, and in order to suppress the exponential growth, the spinorial components $\tilde{\alpha}_i$ have to verify

$$\tilde{\alpha}_1(\varrho_\infty)=-\frac{\bar{m}}{\Omega m_h}\tilde{\alpha}_2(\varrho_\infty)+\frac{m_f}{\Omega m_h}\tilde{\alpha}_4(\varrho_\infty), \tag{34}$$

$$\tilde{\alpha}_3(\varrho_\infty)=-\frac{m_f}{\Omega m_h}\tilde{\alpha}_2(\varrho_\infty)+\frac{\bar{m}}{\Omega m_h}\tilde{\alpha}_4(\varrho_\infty). \tag{35}$$

These conditions constrain two degrees of freedom, and another one is fixed by normalization of the wave functions at ϱ_∞. As a result, only one free parameter can be used yet in order to achieve the matching between these well defined solutions and the two normalizable ones near the string core. It will be the case only for particular values of the mass $\bar{m}$. Numerically, the matching is performed in two steps. First, by means of the last free parameter, one of the usually divergent component near the string core is made to vanish at ϱ $=0$. Obviously, this component is chosen among those having a nonzero winding number since, in order to be single valued by rotation around the vortex, it necessarily vanishes at the string core. Once it is performed, the last divergent component at $\varrho=0$ is regularized, its turn, by calculating the mass of the mode $\bar{m}$ leading to a convergent solution. For the range of model parameters previously defined, the numerical computations thus lead to the mass of the trapped wave solutions as well as their components as function of the radial distance to the string core $\tilde{\alpha}_i(\varrho)$.

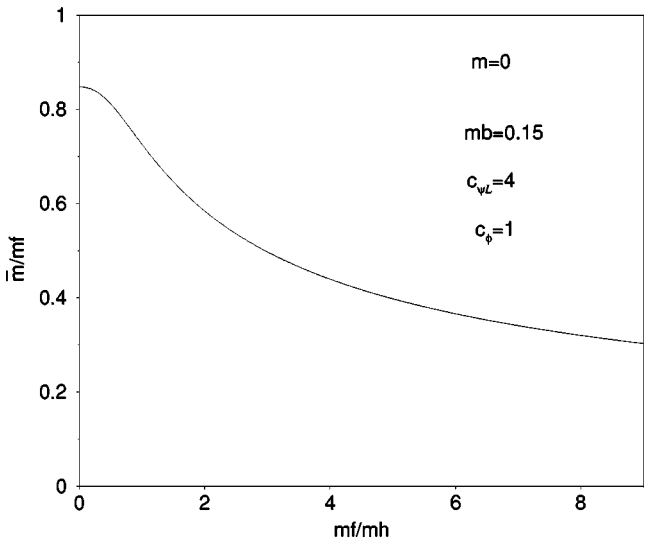

FIG. 2. The mass of the lowest massive bound state, relative to the fermion vacuum mass, plotted as function of the coupling constant to the Higgs field, i.e., the fermion vacuum mass relative to the mass of the Higgs boson.

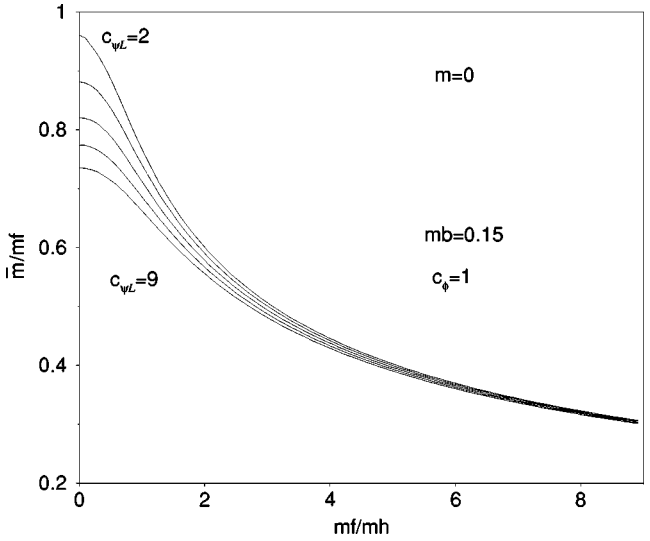

FIG. 3. The mass of the lowest massive bound state, relative to the fermion vacuum mass, plotted as function of the coupling constant to the Higgs field, for several values of the fermionic charges. The closest c_{ψ_L} is to $c_\phi/2$, the higher mode mass $\bar{m}$ is. In the extreme case $c_{\psi_L}\sim c_\phi/2$, $\bar{m}\sim m_f$ there is no longer normalizable massive bound state *in the perturbative sector*.

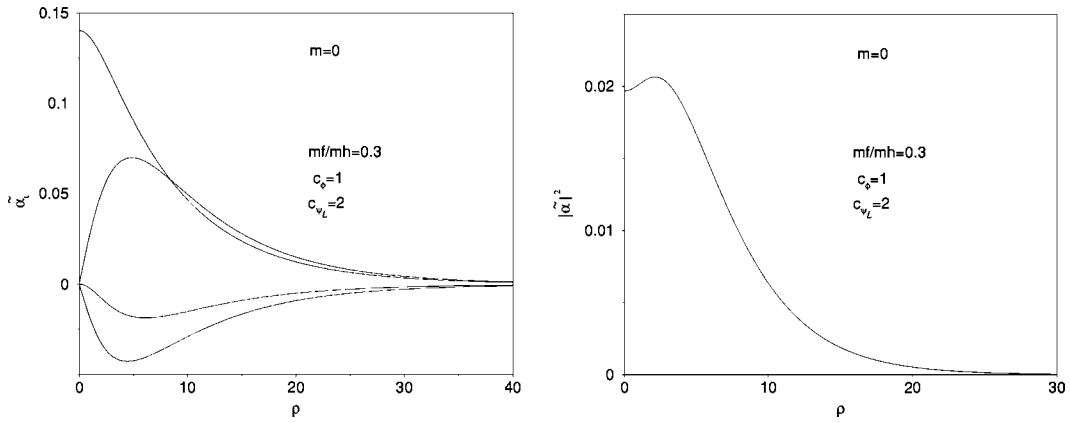

FIG. 4. The transverse spinorial components of the Ψ field, as functions of the distance to the string core, for the lowest massive bound state. The transverse normalized probability density is also plotted and takes its maximum value nearby the string core, as expected for massive bound states exploring the neighborhood of the core by means of nonvanishing angular momentum. Note that for $m=0$, one spinorial component behaves like a zero mode one, i.e., it condenses in the string core contrary to the others.

4. Numerical results

In what follows, the Higgs winding number is assumed fixed to the value $n=1$, and the range of c_{ψ_L} restricted to $c_{\psi_L} \geqslant c_\phi/2$, the other case being derivable from the symmetric properties discussed above.

The first results concern the ''perturbative sector'' where the fermion vacuum mass verifies $m_f < m_h$, or equivalently, for a smaller Yukawa coupling constant than the Higgs self-coupling, i.e., $g < \sqrt{\lambda}$. In this case, for reasonable values of the fermion charges, i.e., of the same order of magnitude than the Higgs one $c_{\psi_L} \gtrsim c_\phi/2$, only one normalizable massive bound state is found with null winding number $m=0$. As a result, by means of transformations (28), there are also symmetric modes for $c_{\psi_L} \leqslant c_\phi/2$, with winding number $m=2$. The dependency of the mode mass $\bar{m}$ with the fermion vacuum mass and charges (i.e., the coupling constants to Higgs and gauge fields) is plotted in Figs. 2 and 3. The study has been also extended to the nonperturbative sector where this massive mode thus appears as the lowest massive bound state. First, it is found that the mass of the trapped mode always decreases with respect to the coupling constant, i.e, with the fermion vacuum mass m_f. Moreover, for small values of m_f/m_h, the derivative of the curve $\bar{m}(m_f/m_h)$ vanishes near the origin (see Fig. 2). As a result, the mass modes in the full perturbative sector does not depend on the coupling constant to the Higgs field, at first order. On the other hand, Fig. 3 shows that the mass of the bound state hardly depends at all on its coupling with the gauge field (i.e., on the charges c_{ψ_L}) in the nonperturbative sector, where all the curves have the same asymptotic behavior. Near the origin, the closest c_{ψ_L} is to $c_\phi/2$, the higher mode mass $\bar{m}$ is. In the particular limiting case $c_{\psi_L} \sim c_\phi/2$, there is no normalizable massive bound state, and as can be seen in Fig. 3, already for $c_{\psi_L}/c_\phi = 2$, the mode mass is close to m_f. It is not surprising since, as it was above noted, $c_{\psi_L} = c_\phi/2$ is a frontier between two kinds of solutions with different winding numbers, and thus, at this point, the ''normalizable'' winding numbers are not well defined. Note that this is only true if $m \neq (n+1)/2$ as it is the case here in the perturbative sector with $n=1$ and $m=0$.

The normalized scaled spinorial components $\tilde{\alpha}(\varrho)$ have been plotted in Fig. 4 for the lowest massive bound state, with the normalization

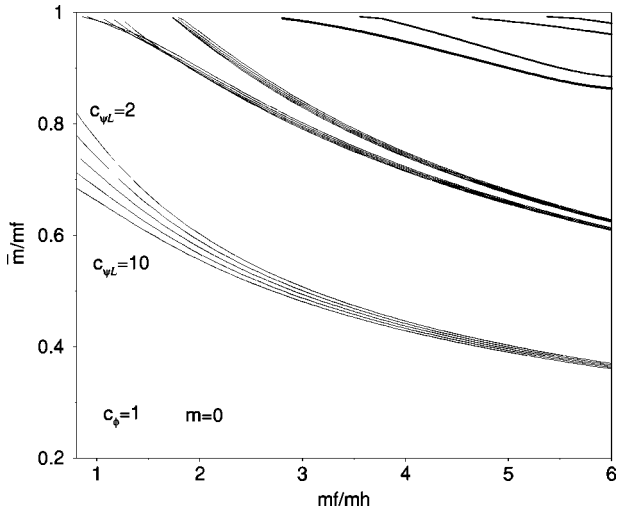

FIG. 5. The evolution of the mass spectrum for $m=0$ winding number, as function of the coupling constants. Each main branch represents one massive mode whereas the substructures show its evolution with respect to the fermion charge c_{ψ_L}. Five values of the fermion charge have been plotted, from $c_{\psi_L}=2$ to $c_{\psi_L}=10$, and the spectrum has been computed only in the nonperturbative sector, since only the lowest mode exists for lower values of m_f/m_h (see Fig. 3). As expected, all the modes have mass $\bar{m}$ decreasing with their coupling constant to the Higgs field. Moreover, the substructures show that, for sufficiently large values of m_f/m_h, the mode mass is a decreasing function of the charge c_{ψ_L}. However, note that this behavior can be inverted for some modes close to their appearance region, as it is the case for the second one.

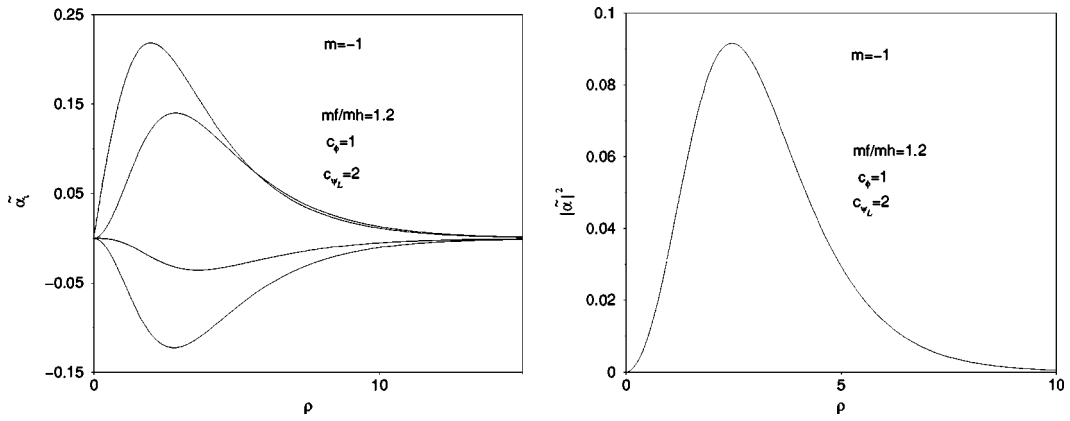

FIG. 6. The transverse spinorial components of the Ψ field, plotted as functions of the distance to the string core, for the $m=-1$ lowest massive bound state. The transverse normalized probability density is also plotted and vanishes in the string core. In this case, all components of the spinor wind around the string and the corresponding mode is thus centrifugally confined in a shell nearby the core, as expected for a nonzero angular momentum eigenstate.

$$\int \varrho \, \mathrm{d}\varrho \, \tilde{\alpha}_i^\dagger \tilde{\alpha}_i = 1. \tag{36}$$

The corresponding transverse probability density has also been plotted in Fig. 4. Note that the massive mode wave function is larger around the string rather on it, as expected for a nonvanishing angular momentum.

The nonperturbative cases with $m_\mathrm{f} > m_\mathrm{h}$, involve much more massive bound states. First, another mode appears in addition to the previous one, with the same winding number.

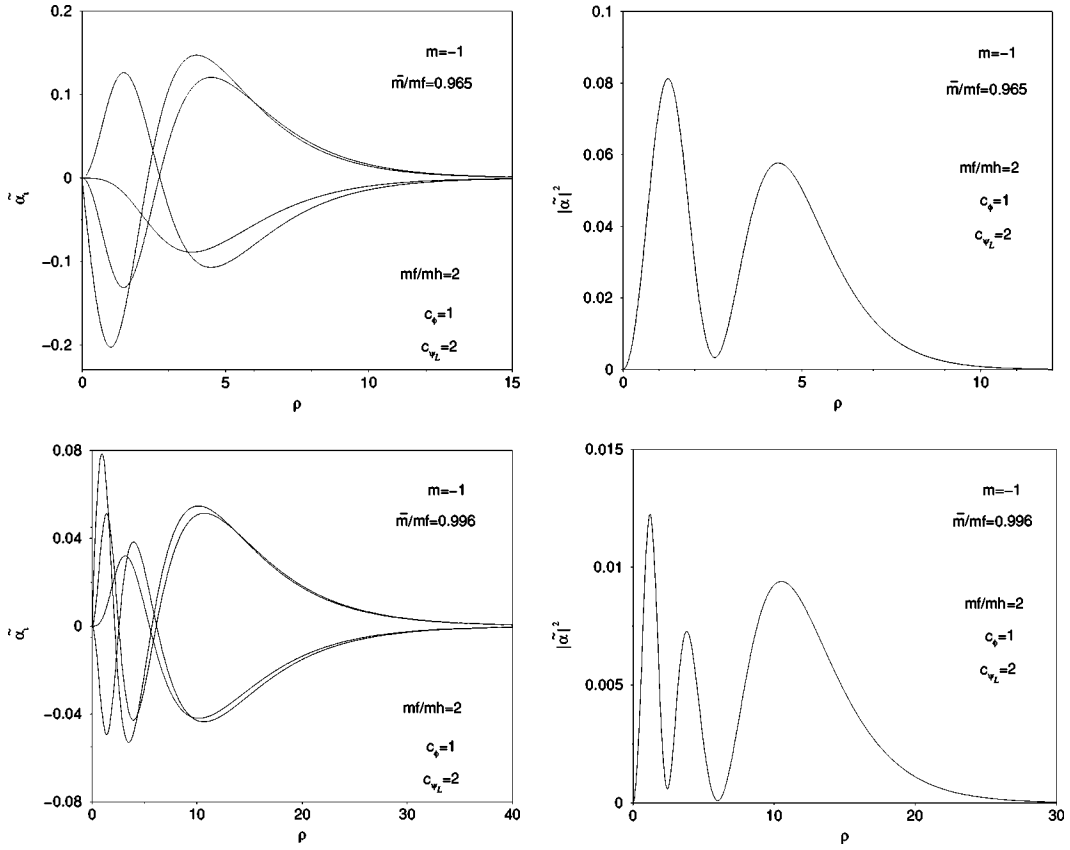

FIG. 7. The components of the Ψ field as function of the radial distance, and the corresponding transverse probability densities. The curves have been computed for $m=-1$ winding number, and for two additional incoming modes in the nonperturbative sector. As expected, interferences fringes appear from the nonzero angular momentum eigenvalues of these modes.

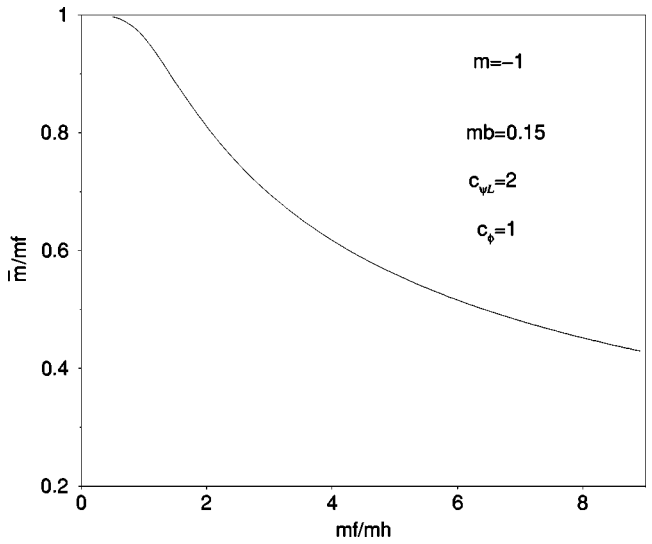

FIG. 8. The mass of the $m=-1$ lowest massive bound state, relative to the fermion vacuum mass, with respect to the coupling constant to the Higgs field. Note that the mode does not exist in the perturbative sector.

Because of the fact that $\bar{m}$ decreases with m_f (see Fig. 2), for higher values of m_f, another mode comes into the normalizable mass range. Since normalizability at infinity requires $\bar{m}<m_f$, the number of massive modes increases with the value of m_f. Moreover, there are also solutions involving all the other possible winding numbers. The evolution of the mass spectrum, for winding number $m=0$, and with respect to the coupling constant to the Higgs and gauge fields is plotted in Fig. 5. The behavior of each mass is the same as that of the lowest mode previously studied, the new properties resulting only in the appearance of new states for higher values of the fermion vacuum mass m_f, as found for two-dimensional Weyl spinors in Ref. [26].

Physically, the additional massive modes at a given winding number can be interpreted as normalizable eigenstates of the angular momentum operator in the vortex potential, with higher eigenvalues. From Figs. 4 and 6, one can see that for each value of m, the lowest massive state is confined around the string with a transverse probability density showing only one peak whereas the higher massive modes have transverse probability density profiles with an increasing number of maxima, as can be seen in Fig. 7. In fact, as for the structure of atomic spectra, the two spatial degrees of freedom of the attractive potential certainly lead to two quantum numbers labeling the observable eigenstates, one of them being clearly m, and the other appearing through the number of zeros of the spinorial components, or, equivalently, the number of maxima of the associated transverse probability density.

The massive modes with higher winding numbers behave in the same way. However, they exist only for nonzero values of the coupling constant m_f/m_h, this one increasing with the value of the winding number m. The scaled spinorial components and the transverse normalized probability density of the lowest massive bound state with next $m=-1$ winding number are plotted in Fig. 6. They are found to be normalizable for coupling constant $m_f/m_h \gtrsim 0.5$ when $c_{\psi_L}/c_\phi=2$, as can be seen in Fig. 8. Contrary to the $m=0$ lowest massive state, all spinorial components wind around the string, and the transverse probability of finding such a mode vanishes in the string core, as expected for a nonzero angular momentum eigenstate. Obviously, this is also true for all higher values of m, as for the $m=-2$ massive mode which appears to be normalizable for $m_f/m_h \gtrsim 1.2$.

It is clear from the numerical results that the fermions can be trapped in the string in the form of massive bound states, for a wide range of model parameters. The only exception takes place for fermion charges close to the particular value $c_{\psi_L}=c_\phi/2$ where there is no normalizable massive bound state in the perturbative sector. Note, again, that all the previous results are also relevant for the massive modes with symmetric winding numbers $\hat{m}=n+1-m$, as well as for the $\mathcal{X}$ spinor field and for the antiparticle states of both Ψ and $\mathcal{X}$ fermions.

IV. FOCK SPACE FOR MASSIVE MODES

The existence of massive trapped waves requires that the quantum state space [25] be enlarged to include them. For each normalizable mode with mass $\bar{m}$, a two-dimensional Fock space can be constructed by spinor field expansion over the relevant massive plane waves. The full quantum theory can therefore be obtained from tensorial product of the different Fock spaces belonging to their own mass representation, together with the Fock space associated with the zero modes [25]. As a first step toward a full theory, we will only consider the plane waves associated with one massive mode of mass $\bar{m}$.

A. Quantum field operators

Quantization is performed through the canonical procedure by defining creation and annihilation operators satisfying anticommutation rules. However, the particular structure of the trapped massive waves yields relationships between longitudinal quantum operators with nontrivial transverse dependencies.

1. Fourier transform

In the previous section, it was shown that the fermions could propagate along the string direction with given mass $\bar{m}$ belonging to the spectrum. From Eq. (17), setting

$$\Psi_p^{(+)}=u_\psi(k,r,\theta)e^{i(\omega t-kz)}, \quad \Psi_p^{(-)}=v_\psi(k,r,\theta)e^{-i(\omega t-kz)}, \tag{37}$$

with

$$\omega=\sqrt{\bar{m}^2+k^2}, \tag{38}$$

and using the symmetry properties shown in Sec. III B 2, the transverse parts of the massive trapped waves for particle and antiparticle states can be written as

$$u_\psi(k,x_\perp)=\begin{pmatrix}\sqrt{\omega+k}\,\overline{\alpha}_1(r)\mathrm{e}^{-im\theta}\\ i\sqrt{\omega-k}\,\overline{\alpha}_2(r)\mathrm{e}^{-i(m-1)\theta}\\ \sqrt{\omega-k}\,\overline{\alpha}_3(r)\mathrm{e}^{-i(m-n)\theta}\\ i\sqrt{\omega+k}\,\overline{\alpha}_4(r)\mathrm{e}^{-i(m-n-1)\theta}\end{pmatrix},$$

$$v_\psi(k,x_\perp)=\begin{pmatrix}\sqrt{\omega+k}\,\overline{\alpha}_1(r)\mathrm{e}^{-im\theta}\\ -i\sqrt{\omega-k}\,\overline{\alpha}_2(r)\mathrm{e}^{-i(m-1)\theta}\\ -\sqrt{\omega-k}\,\overline{\alpha}_3(r)\mathrm{e}^{-i(m-n)\theta}\\ i\sqrt{\omega+k}\,\overline{\alpha}_4(r)\mathrm{e}^{-i(m-n-1)\theta}\end{pmatrix}, \tag{39}$$

with the notations

$$x_\perp=(r,\theta),\quad \text{and}\quad \overline{\alpha}=\frac{m_\mathrm{h}}{\sqrt{2\pi}}\,\tilde{\alpha}. \tag{40}$$

Contrary to the zero mode case, fermions can now propagate in both directions of the string, so that the momentum k of the massive waves can take positive and negative values. As a result, the Ψ field can be Fourier expanded over positive and negative energy states as

$$\Psi=\int\frac{\mathrm{d}k}{2\pi 2\omega}[b^\dagger(k)u(k,x_\perp)\mathrm{e}^{i(\omega t-kz)}+d(k)v(k,x_\perp)\mathrm{e}^{-i(\omega t-kz)}], \tag{41}$$

where the subscripts have been omitted. The normalization convention of the Fourier transform is chosen as in the zero modes case [25], i.e.,

$$\int\mathrm{d}z\,\mathrm{e}^{i(k-k')z}=2\pi\delta(k-k'). \tag{42}$$

Obviously, the $\mathcal{X}$ field verifies similar relations with the transformation $n\to -n$, as was noted previously.

2. Commutation relations

In order to express the Fourier coefficients $b(k)$ and $d^\dagger(k)$ as function of the spinor field Ψ, let us introduce another unit spinors

$$\hat{u}(k,x_\perp)=\begin{pmatrix}\sqrt{\omega+k}\,\overline{\alpha}_3(r)\mathrm{e}^{-im\theta}\\ i\sqrt{\omega-k}\,\overline{\alpha}_4(r)\mathrm{e}^{-i(m-1)\theta}\\ \sqrt{\omega-k}\,\overline{\alpha}_1(r)\mathrm{e}^{-i(m-n)\theta}\\ i\sqrt{\omega+k}\,\overline{\alpha}_2(r)\mathrm{e}^{-i(m-n-1)\theta}\end{pmatrix},$$

$$\hat{v}(k,x_\perp)=\begin{pmatrix}\sqrt{\omega+k}\,\overline{\alpha}_3(r)\mathrm{e}^{-im\theta}\\ -i\sqrt{\omega-k}\,\overline{\alpha}_4(r)\mathrm{e}^{-i(m-1)\theta}\\ -\sqrt{\omega-k}\,\overline{\alpha}_1(r)\mathrm{e}^{-i(m-n)\theta}\\ i\sqrt{\omega+k}\,\overline{\alpha}_2(r)\mathrm{e}^{-i(m-n-1)\theta}\end{pmatrix}. \tag{43}$$

They clearly verify $\hat{u}=\gamma^0\gamma^3\hat{v}$ and from Eq. (39)

$$\hat{u}^\dagger(k)u(k)=\hat{v}^\dagger(k)v(k)=2\omega\,\overline{\nu}(r),\qquad \hat{u}(k)^\dagger v(-k)=\hat{v}^\dagger(k)u(-k)=0, \tag{44}$$

where the dependency with respect to transverse coordinates have been omitted in order to simplify the notation, and where we introduced the function

$$\overline{\nu}(r)=\overline{\alpha}_1(r)\overline{\alpha}_3(r)+\overline{\alpha}_2(r)\overline{\alpha}_4(r). \tag{45}$$

From Eqs. (41), (42), and (44), the Fourier coefficients are found to be functions of the Ψ field, and read

$$b^\dagger(k)=\frac{1}{\mathcal{N}}\int r\,\mathrm{d}r\,\mathrm{d}\theta\,\mathrm{d}z\,\mathrm{e}^{-i(\omega t-kz)}\hat{u}^\dagger(k,x_\perp)\Psi,\qquad d(k)=\frac{1}{\mathcal{N}}\int r\,\mathrm{d}r\,\mathrm{d}\theta\,\mathrm{d}z\,\mathrm{e}^{i(\omega t-kz)}\hat{v}^\dagger(k,x_\perp)\Psi, \tag{46}$$

where we have defined the normalization factor

$$\mathcal{N}=\int r\,\mathrm{d}r\,\mathrm{d}\theta\,\overline{\nu}(r)=\int\varrho\,\mathrm{d}\varrho\,\tilde{\nu}(\varrho). \tag{47}$$

Similarly, the expansion of the $\Psi^\dagger$ field on the same positive and negative energy solutions leads to the definition of its Fourier coefficients, namely $b(k)$ and $d^\dagger(k)$. From Eqs. (42) and (44), they can also be expressed as functions of $\Psi^\dagger$, and verify

$$b(k)=[b^\dagger(k)]^\dagger,\quad \text{and}\quad d^\dagger(k)=[d(k)]^\dagger. \tag{48}$$

In order to perform a canonical quantization along the string world sheet, let us postulate the anticommutation rules, *at equal times*, between the spinor fields

$$\{\Psi_i(t,\vec{x}),\Psi^{\dagger j}(t,\vec{x'})\}=\delta(z-z')(\Gamma^0)_i^j(x_\perp,x'_\perp), \tag{49}$$

where Γ^0 is a matrix with respect to spinor components whose utility will be justified later, and which reads

$$\Gamma^0(x_\perp,x'_\perp)=\frac{1}{2\overline{m}^2}(\omega\mathrm{I}-k\gamma^0\gamma^3)[u(k,x_\perp)u^\dagger(k,x'_\perp)+v(k,x_\perp)v^\dagger(k,x'_\perp)]. \tag{50}$$

Note that Γ^0 does not depend on ω and k. Explicit calculations show that the first terms involving ω and k are mixed with $u(k)$ and $v(k)$, and yield Lorentz invariant quantities, such as $\overline{m}$. Moreover, Γ^0 has the following orthonormalization properties

$$\hat{u}^\dagger(k,x_\perp)\Gamma^0(x_\perp,x'_\perp)\hat{u}(k,x'_\perp)=2\omega\,\overline{\nu}(r)\overline{\nu}(r'),\qquad \hat{u}^\dagger(k,x_\perp)\Gamma^0(x_\perp,x'_\perp)\hat{v}(-k,x'_\perp)=0, \tag{51}$$

and similar relationships are obtained for $\hat{v}$ by swapping $\hat{u}$ and $\hat{v}$.

The anticommutation rules for the Ψ Fourier coefficients are immediately obtained from Eqs. (42), (46), (48), and Eq. (49), using the properties of Γ^0 in Eq. (51), and read

$$\{b(k),b^\dagger(k')\}=\{d(k),d^\dagger(k')\}=2\pi 2\omega\delta(k-k'), \tag{52}$$

with all the other anticommutators vanishing. As a result, the Fourier coefficients $b^\dagger$ and $d^\dagger$ behave as well defined creation operators, whereas their complex conjugates, b and d, act as annihilation operators of a particle and antiparticle massive state, respectively.

In order to verify the microcausality of the theory and to justify, *a posteriori*, the ansatz of Eq. (49), let us derive the anticommutator between the quantum field operators Ψ and $\Psi^\dagger$, *at any time*. The Ψ expansion in Eq. (41) and its complex conjugate yield

$$\begin{aligned}\{\Psi_i(\mathbf{x}),\Psi^{\dagger j}(\mathbf{x}')\}=\int\frac{dk\,dk'}{(2\pi)^2 2\omega 2\omega'}&\\ \times[\{b^\dagger(k),b(k')\}u_i(k,x_\perp)u^{\dagger j}(k',x'_\perp)&\\ \times e^{i[(\omega t-\omega' t')-(kz-k'z')]}&\\ +\{d(k),d^\dagger(k')\}v_i(k,x_\perp)v^{\dagger j}(k',x'_\perp)&\\ \times e^{-i[(\omega t-\omega' t')-(kz-k'z')]}].&\end{aligned} \tag{53}$$

Using Eq. (52), this equation simplifies to involve tensorial products of unit spinors evaluated at the same momentum. It is therefore convenient to introduce two additional matrices, namely $\Gamma^3(x_\perp,x'_\perp)$ and $\mathcal{M}(x_\perp,x'_\perp)$, which verify

$$\begin{aligned}u(k,x_\perp)u^\dagger(k,x'_\perp)&=\omega\Gamma^0(x_\perp,x'_\perp)-k\Gamma^3(x_\perp,x'_\perp)\\ &\quad-\mathcal{M}(x_\perp,x'_\perp),\\ v(k,x_\perp)v^\dagger(k,x'_\perp)&=\omega\Gamma^0(x_\perp,x'_\perp)-k\Gamma^3(x_\perp,x'_\perp)\\ &\quad+\mathcal{M}(x_\perp,x'_\perp).\end{aligned} \tag{54}$$

From Eq. (39), these matrices are simply related to Γ^0 by

$$\begin{aligned}\Gamma^3(x_\perp,x'_\perp)&=\Gamma^0(x_\perp,x'_\perp)\gamma^3\gamma^0,\\ \mathcal{M}(x_\perp,x'_\perp)&=\Gamma^0(x_\perp,x'_\perp)\mathcal{M}_{\rm d}(x'_\perp)\gamma^0,\end{aligned} \tag{55}$$

where $\mathcal{M}_{\rm d}(x_\perp)$ is the diagonal matrix

$$\begin{aligned}\mathcal{M}_{\rm d}(x_\perp)=\overline{m}\,\mathrm{Diag}\Bigg(\frac{\overline{\alpha_3}(r)}{\overline{\alpha_1}(r)}e^{-in\theta},\frac{\overline{\alpha_4}(r)}{\overline{\alpha_2}(r)}e^{-in\theta},\frac{\overline{\alpha_1}(r)}{\overline{\alpha_3}(r)}&\\ \times e^{in\theta},\frac{\overline{\alpha_2}(r)}{\overline{\alpha_4}(r)}e^{in\theta}\Bigg).&\end{aligned} \tag{56}$$

From Eqs. (54) and (55), the anticommutator (53) reduces to

$$\begin{aligned}\{\Psi(\mathbf{x}),\Psi^\dagger(\mathbf{x}')\}=[\Gamma^0(x_\perp,x'_\perp)i\partial_0+\Gamma^3(x_\perp,x'_\perp)i\partial_3&\\ +\mathcal{M}(x_\perp,x'_\perp)]i\Delta(x_\parallel-x'_\parallel),&\end{aligned} \tag{57}$$

where $x_\parallel=(t,z)$, and Δ is the well-known Pauli Jordan function which reads

$$i\Delta(x_\parallel-x'_\parallel)=\int\frac{dk}{2\pi 2\omega}[e^{-ik(x_\parallel-x'_\parallel)}-e^{ik(x_\parallel-x'_\parallel)}], \tag{58}$$

and vanishes outside the light cone. As a result, the quantum fields indeed respect microcausality along the string. The matrices Γ^μ appear as the analogues of the matrices γ^μ for the Dirac spinors living in the vortex. The two-dimensional quantization along the string is thus not independent of the transverse structure. It is all the more manifest in the anticommutator expression between Ψ and $\overline{\Psi}$: from Eq. (57), and using Eq. (55), one gets

$$\begin{aligned}\{\Psi(\mathbf{x}),\overline{\Psi}(\mathbf{x}')\}=\Gamma^0(x_\perp,x'_\perp)[i\gamma^0\partial_0+i\gamma^3\partial_3&\\ +\mathcal{M}_{\rm d}(x'_\perp)]i\Delta(x_\parallel-x'_\parallel).&\end{aligned} \tag{59}$$

The matrix Γ^0 now appears clearly as a local transverse normalization of the longitudinal quantum field operators. Note that the mass term also depends on the transverse coordinates due to the nontrivial profile of the Higgs field around the string. Moreover, setting $t=t'$ in Eq. (57), leads to the postulated anticommutator at equal times (49), and therefore justifies the introduction of the Γ^0 term.

3. Fock states

In the following, $|\mathcal{P}\rangle$ will design a Fock state constructed by applying creation operators associated with a massive mode $\overline{m}$, on the relevant string vacuum. Such a state was similarly defined for zero modes in Ref. [25]. From the anticommutators (52), a massive Ψ state with momentum k is now normalized according to

$$\langle k'|k\rangle=2\pi 2\omega\delta(k-k'). \tag{60}$$

Similarly, it will turn out to be convenient to derive the average of the occupation number operator since it will appear in the derivation of the equation of state. From Eq. (52), and for a Ψ massive mode, it reads

$$\frac{\langle\mathcal{P}|b^\dagger(k)b(k')|\mathcal{P}\rangle}{\langle\mathcal{P}|\mathcal{P}\rangle}=\frac{2\pi}{L}2\omega 2\pi\sum_i\delta(k-k_i)\delta(k'-k_i), \tag{61}$$

where the summation runs over all Ψ massive particle states present in the relevant $\overline{m}$ Fock state $|\mathcal{P}\rangle$, and L is the physical string length, coming from the $\delta(0)$ regularization by means of Eq. (42).

B. Stress tensor and Hamiltonian

The classical stress tensor can immediately be derived from variation of the full Lagrangian (1) with respect to the metric, and the Ψ fermionic part thus reads [25]

$$T^{\mu\nu}_\psi=\frac{i}{2}\overline{\Psi}\gamma^{(\mu}\partial^{\nu)}\Psi-\frac{i}{2}[\partial^{(\mu}\overline{\Psi}]\gamma^{\nu)}\Psi-B^{(\mu}j^{\nu)}_\psi. \tag{62}$$

1. Hamiltonian

The quantum operators associated with the classically conserved charges can be obtained by replacing the classical fields by their quantum forms involving creation and annihilation operators. In this way, the Hamiltonian appears, from Noether theorem, as the charge associated with the time component of the energy momentum tensor

$$T^{tt}_{\psi}=i\overline{\Psi}\gamma^0\partial_t\Psi-i(\partial_t\overline{\Psi})\gamma^0\Psi. \tag{63}$$

Using Eqs. (39) and (41) in the previous equation, and performing a spatial integration, the Hamiltonian operator reads, after some algebra,

$$P^t_{\psi}=\int\frac{\mathrm{d}k}{2\pi 2\omega}\int\mathrm{d}^2x_{\perp}[-b(k)b^{\dagger}(k)+d^{\dagger}(k)d(k)]\overline{u}(k,x_{\perp})\gamma^0u(k,x_{\perp}). \tag{64}$$

In order to simplify this expression, let us introduce the parameters

$$\overline{\Sigma}^2_{\mathrm{X}}=\overline{\alpha}^2_2+\overline{\alpha}^2_3,\quad\text{and}\quad\overline{\Sigma}^2_{\mathrm{Y}}=\overline{\alpha}^2_1+\overline{\alpha}^2_4. \tag{65}$$

From Eq. (39), the Hamiltonian now reads

$$P^t_{\psi}=\int\frac{\mathrm{d}k}{2\pi 2\omega}[-b(k)b^{\dagger}(k)+d^{\dagger}(k)d(k)][(\omega-k)||\Sigma^2_{\mathrm{X}}||+(\omega+k)||\Sigma^2_{\mathrm{Y}}||], \tag{66}$$

with

$$||\Sigma^2||=\int r\,\mathrm{d}r\,\mathrm{d}\theta\,\overline{\Sigma}^2=\int\varrho\,\mathrm{d}\varrho\,\tilde{\Sigma}^2(\varrho). \tag{67}$$

Analogous relations also hold for the $\mathcal{X}$ field. It is interesting to note that Eq. (66) generalizes the expression previously derived in the zero modes case [25], being found again by setting $\omega=-k$ for the Ψ zero modes, or $\omega=k$ for the $\mathcal{X}$ ones. The normal ordered Hamiltonian is obtained if one uses the anticommuting normal ordered product for creation and annihilation operators, i.e.,

$$:P^t_{\psi}:=\int\frac{\mathrm{d}k}{2\pi 2\omega}[b^{\dagger}(k)b(k)+d^{\dagger}(k)d(k)][(\omega-k)||\Sigma^2_{\mathrm{X}}||+(\omega+k)||\Sigma^2_{\mathrm{Y}}||]. \tag{68}$$

Since $\omega\geqslant k$, this Hamiltonian is always positive definite and is thus well defined. Note that, as in the zero mode case, such a prescription overlooks the energy density difference between the vacuum on the string and the usual one, but it can be shown to vary as $1/L^2$ and therefore goes to zero in the infinite string limit [25,30,31].

2. Effective stress tensor

In order to make contact with the macroscopic formalism [14], it is necessary to express the classically observable quantities with no explicit dependence in the microscopic structure. The relevant two-dimensional fermionic energy momentum tensor can be identified with the full one in Eq. (62), once the transverse coordinates have been integrated over. Due to the cylindrical symmetry around the string direction, z say, all nondiagonal components, in a Cartesian basis, involving a transverse coordinate vanish after integration. Moreover, since the fermion fields are normalizable in the transverse plane, the diagonal terms, $T^{rr}_{\mathcal{F}}$ and $T^{\theta\theta}_{\mathcal{F}}$, are also well defined, and by means of local transverse stress tensor conservation, the integrated diagonal components, $T^{xx}_{\mathcal{F}}$ and $T^{yy}_{\mathcal{F}}$, also vanish [19]. As expected, the only relevant terms in the macroscopic formalism are thus $T^{\alpha\beta}_{\mathcal{F}}$ with $\alpha,\beta\in\{t,z\}$, i.e., the ones that live only in the string world sheet. On the other hand, the macroscopic limit of the involved quantum operators is simply obtained by taking their average over the relevant Fock states.

Replacing the quantum fields in Eq. (62) by their expansion (41), and using Eq. (39), one gets the quantum expression of the energy momentum tensor. Averaging the relevant components $T^{\alpha\beta}_{\psi}$ in the Fock state $|\mathcal{P}\rangle$, by means of Eqs. (39) and (61), one obtains

$$\langle:T^{tt}_{\psi}:\rangle_{\mathcal{P}}=\frac{1}{L}\left[\sum_i^{N_{\psi}}\overline{u}(k_i)\gamma^0u(k_i)+\sum_j^{\overline{N}_{\psi}}\overline{u}(k_j)\gamma^0u(k_j)\right], \tag{69}$$

$$\langle:T^{zz}_{\psi}:\rangle_{\mathcal{P}}=\frac{1}{L}\left[\sum_i^{N_{\psi}}\frac{k_i}{\omega_i}\overline{u}(k_i)\gamma^3u(k_i)+\sum_j^{\overline{N}_{\psi}}\frac{k_j}{\omega_j}\overline{u}(k_j)\gamma^3u(k_j)\right], \tag{70}$$

$$\langle:T^{tz}_{\psi}:\rangle_{\mathcal{P}}=\frac{1}{2L}\left(\sum_i^{N_{\psi}}\left[\overline{u}(k_i)\gamma^3u(k_i)+\frac{k_i}{\omega_i}\overline{u}(k_i)\gamma^0u(k_i)\right]+(i,N_{\psi})\leftrightarrow(j,\overline{N}_{\psi})\right), \tag{71}$$

where the i summations run over the N_{ψ} particle states with momentum k_i involved in the Fock state $|\mathcal{P}\rangle$, while the j summations take care of the $\overline{N}_{\psi}$ antiparticle states with momentum k_j, all with mass $\overline{m}$. In order to simplify the notation, the transverse dependence of the unit spinors have not been written, and the averaged operators stand for

$$\langle T^{\alpha\beta}\rangle_{\mathcal{P}}=\frac{\langle\mathcal{P}|T^{\alpha\beta}|\mathcal{P}\rangle}{\langle\mathcal{P}|\mathcal{P}\rangle}. \tag{72}$$

Similarly, the same relationships can be derived for the $\mathcal{X}$ field, by replacing the Ψ unit spinors by the $\mathcal{X}$ ones with the correct angular dependence, and certainly, in another mass representation $\overline{m}_{\chi}$. Once the transverse coordinates have been integrated over, Eqs. (69), (70), and (71), lead to the two-dimensional Ψ stress tensor.

$$\langle \overline{T}^{\alpha\beta}_{\psi} \rangle_{\mathcal{P}} = \begin{pmatrix} E_{\psi_{\mathcal{P}}} ||\Sigma^2_{\rm Y}|| + \overline{E}_{\psi_{\mathcal{P}}} ||\Sigma^2_{\rm X}|| & \dfrac{E_{\psi_{\mathcal{P}}} + P_{\psi_{\mathcal{P}}}}{2} ||\Sigma^2_{\rm Y}|| - \dfrac{\overline{E}_{\psi_{\mathcal{P}}} - \overline{P}_{\psi_{\mathcal{P}}}}{2} ||\Sigma^2_{\rm X}|| \\ \dfrac{E_{\psi_{\mathcal{P}}} + P_{\psi_{\mathcal{P}}}}{2} ||\Sigma^2_{\rm Y}|| - \dfrac{\overline{E}_{\psi_{\mathcal{P}}} - \overline{P}_{\psi_{\mathcal{P}}}}{2} ||\Sigma^2_{\rm X}|| & P_{\psi_{\mathcal{P}}} ||\Sigma^2_{\rm Y}|| - \overline{P}_{\psi_{\mathcal{P}}} ||\Sigma^2_{\rm X}|| \end{pmatrix}, \tag{73}$$

with the notations

$$\begin{aligned} E_{\psi_{\mathcal{P}}} &= \frac{1}{L}\left[\sum_i^{N_\psi} (\omega_i + k_i) + \sum_j^{\overline{N}_\psi} (\omega_j + k_j) \right], \\ \overline{E}_{\psi_{\mathcal{P}}} &= \frac{1}{L}\left[\sum_i^{N_\psi} (\omega_i - k_i) + \sum_j^{\overline{N}_\psi} (\omega_j - k_j) \right], \\ P_{\psi_{\mathcal{P}}} &= \frac{1}{L}\left[\sum_i^{N_\psi} \frac{k_i}{\omega_i}(\omega_i + k_i) + \sum_j^{\overline{N}_\psi} \frac{k_j}{\omega_j}(\omega_j + k_j) \right], \\ \overline{P}_{\psi_{\mathcal{P}}} &= \frac{1}{L}\left[\sum_i^{N_\psi} \frac{k_i}{\omega_i}(\omega_i - k_i) + \sum_j^{\overline{N}_\psi} \frac{k_j}{\omega_j}(\omega_j - k_j) \right]. \end{aligned} \tag{74}$$

Recall that the full effective energy momentum tensor also involves the Higgs and gauge fields of the vortex background. Since they essentially describe a Goto-Nambu string [32], their transverse integration yields a traceless diagonal tensor

$$\int r\, {\rm d}r\, {\rm d}\theta (T^{tt}_{\rm g} + T^{tt}_{\rm h}) = -\int r\, {\rm d}r\, {\rm d}\theta (T^{zz}_{\rm g} + T^{zz}_{\rm h}) \equiv M^2. \tag{75}$$

Note that the full stress tensor may also involve several massive Ψ and $\mathcal{X}$ states, with different masses belonging to the spectrum. In this case, there will be as many additional terms in the form of Eq. (73), as different massive states there are in the chosen Fock states.

C. Fermionic currents

The quantum current operators can be derived from their classical expressions (14) by using Eq. (41), while the corresponding conserved charges are obtained from their spatial integration. By means of Eq. (61), the current operator, averaged in the relevant Fock state $|\mathcal{P}\rangle$, reads

$$\begin{aligned} \langle :j^{\alpha}_{\mathcal{F}}: \rangle_{\mathcal{P}} = {} & q \frac{c_{\mathcal{F}_{\rm R}} + c_{\mathcal{F}_{\rm L}}}{2} \frac{1}{L}\left[-\sum_i^{N_\mathcal{F}} \frac{\overline{u}_i \gamma^\alpha u_i}{\omega_i} + \sum_j^{\overline{N}_\mathcal{F}} \frac{\overline{u}_j \gamma^\alpha u_j}{\omega_j} \right] \\ & + q \frac{c_{\mathcal{F}_{\rm R}} - c_{\mathcal{F}_{\rm L}}}{2} \frac{1}{L}\left[-\sum_i^{N_\mathcal{F}} \frac{\overline{u}_i \gamma^\alpha \gamma_5 u_i}{\omega_i} \right. \\ & \left. + \sum_j^{\overline{N}_\mathcal{F}} \frac{\overline{u}_j \gamma^\alpha \gamma_5 u_j}{\omega_j} \right], \end{aligned} \tag{76}$$

with $\alpha \in \{t,z\}$, and once again, the sums run over Ψ, or $\mathcal{X}$, particle and antiparticle states. The u_i are the unit spinors associated with the field dealt with. Concerning the transverse components, due to the properties of the unit spinors u and v in Eq. (39), only the orthoradial one does not vanish and reads

$$\begin{aligned} \langle :j^{\theta}_{\mathcal{F}}: \rangle_{\mathcal{P}} = {} & -q \frac{c_{\mathcal{F}_{\rm R}} + c_{\mathcal{F}_{\rm L}}}{2} \frac{1}{L}\left[\sum_i^{N_\mathcal{F}} \frac{\overline{u}_i \gamma^\theta u_i}{\omega_i} + \sum_j^{\overline{N}_\mathcal{F}} \frac{\overline{u}_j \gamma^\theta u_j}{\omega_j} \right] \\ & - q \frac{c_{\mathcal{F}_{\rm R}} - c_{\mathcal{F}_{\rm L}}}{2} \frac{1}{L}\left[\sum_i^{N_\mathcal{F}} \frac{\overline{u}_i \gamma^\theta \gamma_5 u_i}{\omega_i} + \sum_j^{\overline{N}_\mathcal{F}} \frac{\overline{u}_j \gamma^\theta \gamma_5 u_j}{\omega_j} \right], \end{aligned} \tag{77}$$

whereas $\langle :j^r_{\mathcal{F}}: \rangle = 0$ due to the bound state nature of the studied currents. As expected, the gauge charges carried by each trapped fermion in the form of massive mode, generate only macroscopic charge and current densities along the string, as was the case for the zero modes [25]. However, the nonvanishing orthoradial component shows that the local charges also wind around the string while propagating in the z direction, as suggested by the above numerical studies. However, this component will be no longer relevant in the macroscopic formalism, since it vanishes in a Cartesian basis, once the transverse coordinates have been integrated over.

Nevertheless, this nonzero angular momentum of the massive modes is found to generate new properties for the longitudinal currents. Let us focus on the vectorial gauge currents generated by one exitation state, with energy ω and momentum k, of a Ψ massive mode, $\overline{m}$ say. From Eq. (76), using Eqs. (39) and (65), the world sheet vectorial charge current reads

$$\langle :j^0_{\psi {\rm V}}: \rangle_{\varepsilon} = -q \frac{c_{\psi_{\rm R}} + c_{\psi_{\rm L}}}{2} \frac{\varepsilon}{L}\left[\left(1 + \frac{k}{\omega}\right) \overline{\Sigma}^2_{\rm Y} + \left(1 - \frac{k}{\omega}\right) \overline{\Sigma}^2_{\rm X} \right], \tag{78}$$

$$\langle :j^3_{\psi {\rm V}}: \rangle_{\varepsilon} = -q \frac{c_{\psi_{\rm R}} + c_{\psi_{\rm L}}}{2} \frac{\varepsilon}{L}\left[\left(1 + \frac{k}{\omega}\right) \overline{\Sigma}^2_{\rm Y} - \left(1 - \frac{k}{\omega}\right) \overline{\Sigma}^2_{\rm X} \right], \tag{79}$$

where $\varepsilon = \pm 1$ stands a one particle or antiparticle exitation state. Now, even setting $k=0$ in the previous equations yields a nonvanishing spatial current. Physically, it can be simply interpreted as an anomalous magneticlike moment of the considered massive mode in its rest frame. Examining Eq. (79) shows that it could be null only if $\overline{\Sigma}^2_{\rm Y}(r) = \overline{\Sigma}^2_{\rm X}(r)$, which is generally not satisfied due to the particular shapes

of massive spinor components trapped in the string (see Sec. III). These ones being associated with nonzero winding numbers, it is therefore not surprising that, even for a massive stationary state along the string, the nonvanishing charge angular momentum around the string generates such additional magneticlike moment. Note that it does not concern the zero modes, first because they precisely involve vanishing winding numbers [25], and then because for them, there is no defined rest frame due to their vanishing mass. Obviously, this property can be generalized for the axial part of the current, and thus is also valid for the total current of any massive spinor field trapped in the string.

All the above construction of the Fock space and the derivation of the quantum operators associated with the energy momentum tensor and gauge currents remains valid for each Ψ and $\mathcal{X}$ massive mode. More precisely, the other masses belonging to the Ψ spectrum verify analogous relationships provided $\overline{m}$ is replaced by the relevant one, as for the unit spinors. In addition, the $\mathcal{X}$ massive states require to transform $n \to -n$ in Eq. (56), due to their coupling to the antivortex. At this stage, the averaged values of the stress tensor and currents have been obtained, and therefore allow the derivation of an equation of state, once the Fock states are known.

V. EQUATION OF STATE

The energy per unit length and tension in a given Fock state $|\mathcal{P}\rangle$ are basically the eigenvalues associated with timelike and spacelike eigenvectors of the effective two-dimensional full stress tensor. Obviously this one includes the classical Goto-Nambu term resulting of the string forming Higgs and gauge fields [see Eq. (75)], with the fermionic part generated by the massive currents [see Eq. (73)]. Moreover, in order to describe the string by an adequate macroscopic formalism, it is necessary to choose a quantum statistics for the relevant Fock states, and for energy scales far below the ones where the string was formed, it is reasonable to consider a Fermi-Dirac distribution at zero temperature [25,33]. In the following, the equation of state is first derived for the lowest massive modes associated with the Ψ and $\mathcal{X}$ field, and simplified in the zero-temperature and infinite string limit. As a second step, these derivations are generalized to any number and kind of trapped fermionic mode.

A. Lowest massive modes

1. Energy per unit length and tension

In this section, we will only consider the lowest massive modes belonging to the Ψ and $\mathcal{X}$ mass spectrums, with masses $\overline{m}_\psi$ and $\overline{m}_\chi$, respectively. From Eqs. (73) and (75), the full effective energy momentum tensor reads

$$\langle \overline{T}^{\alpha\beta} \rangle_{\mathcal{P}} = \int r \, \mathrm{d}r \, \mathrm{d}\theta (T_{\mathrm{g}}^{\alpha\beta} + T_{\mathrm{h}}^{\alpha\beta}) + \langle \overline{T}_{\psi}^{\alpha\beta} \rangle_{\mathcal{P}} + \langle \overline{T}_{\chi}^{\alpha\beta} \rangle_{\mathcal{P}}, \tag{80}$$

where $\overline{T}_{\chi}^{\alpha\beta}$ takes the same form as $\overline{T}_{\psi}^{\alpha\beta}$ in Eqs. (73) and (74) once the Ψ relevant parameters have been replaced by the $\mathcal{X}$ ones. In the preferred frame where the stress tensor is diagonal, we can identify its timelike and spacelike eigenvalues with energy per unit length U and tension T. Upon using Eqs. (73), (75), and (80), these read

$$\begin{aligned} U_{\mathcal{P}} = M^2 + \sum_{\mathcal{F} \in \{\Psi, \mathcal{X}\}} \left[\frac{E_{\mathcal{F}} - P_{\mathcal{F}}}{2} ||\Sigma_{\mathrm{Y}\mathcal{F}}^2|| + \frac{\overline{E}_{\mathcal{F}} + \overline{P}_{\mathcal{F}}}{2} ||\Sigma_{\mathrm{X}\mathcal{F}}^2|| \right] \\ + \left[\sum_{\mathcal{F} \in \{\Psi, \mathcal{X}\}} (E_{\mathcal{F}} + P_{\mathcal{F}}) ||\Sigma_{\mathrm{Y}\mathcal{F}}^2|| \right. \\ \left. \times \sum_{\mathcal{F} \in \{\Psi, \mathcal{X}\}} (\overline{E}_{\mathcal{F}} - \overline{P}_{\mathcal{F}}) ||\Sigma_{\mathrm{X}\mathcal{F}}^2|| \right]^{1/2}, \end{aligned} \tag{81}$$

for the energy per unit length, and

$$\begin{aligned} T_{\mathcal{P}} = M^2 + \sum_{\mathcal{F} \in \{\Psi, \mathcal{X}\}} \left[\frac{E_{\mathcal{F}} - P_{\mathcal{F}}}{2} ||\Sigma_{\mathrm{Y}\mathcal{F}}^2|| + \frac{\overline{E}_{\mathcal{F}} + \overline{P}_{\mathcal{F}}}{2} ||\Sigma_{\mathrm{X}\mathcal{F}}^2|| \right] \\ - \left[\sum_{\mathcal{F} \in \{\Psi, \mathcal{X}\}} (E_{\mathcal{F}} + P_{\mathcal{F}}) ||\Sigma_{\mathrm{Y}\mathcal{F}}^2|| \right. \\ \left. \times \sum_{\mathcal{F} \in \{\Psi, \mathcal{X}\}} (\overline{E}_{\mathcal{F}} - \overline{P}_{\mathcal{F}}) ||\Sigma_{\mathrm{X}\mathcal{F}}^2|| \right]^{1/2}, \end{aligned} \tag{82}$$

for the tension. It is interesting to note first that $U_{\mathcal{P}} + T_{\mathcal{P}} \neq 2M^2$, and thus the fixed trace equation of state previously found for zero modes [25,33] is no longer verified by massive modes, as expected since they are no longer eigenstates of the $\gamma^0 \gamma^3$ operator. Moreover, the expression of energy density and tension does not seem to involve the conserved charge current magnitude, which played the role of a state parameter in the case of a scalar condensate in a cosmic string [14,15]. In fact, as it was the case at zeroth order for the zero modes [25], the charge currents are only involved in the stress tensor through their coupling to the gauge field [see Eq. (62)]. At zeroth order, when the back reaction is neglected, the only nonvanishing component of the gauge field is B_θ, and it therefore couples only with $j_{\mathcal{F}}^{\theta}$, which vanishes once the transverse coordinates have been integrated over. As a result, it is not surprising that the equation of state does not involve the fermionic currents without back reaction. As a result, it is more natural from quantization to define the occupation numbers of the involved species as state parameters.

2. Zero-temperature and infinite string limit

Assuming a Fermi-Dirac distribution at zero temperature for the exitation states, the sums involved in Eq. (74) run over the successive values of the allowed momentum k_i until the Fermi level of the considered species is reached. With periodic boundary conditions on spinor fields, the allowed momentum exitation values are discretized according to

$$k_n = \frac{2\pi}{L} n, \tag{83}$$

where n is an integer, playing the role of a quantum exitation number. As a result, in the relevant $\bar{m}$ representation of each field, the exitation energies ω_i are also discrete according to Eq. (38), and for the Ψ field, the parameters E_ψ and P_ψ in Eq. (74) simplify to sums of radical function of n, with n running from the vacuum to the last filled state. In order to express them as explicit functions of the relevant Fermi level, it is convenient to consider the infinite string limit $L \to \infty$. In this limit one gets

$$\lim_{L\to\infty} \frac{1}{L} \sum_{i=-N_\psi^-}^{N_\psi^+} f(k_i) = \frac{1}{2\pi} \int_{-2\pi\rho_\psi^-}^{2\pi\rho_\psi^+} dk\, f(k), \tag{84}$$

where $\rho_\psi^\pm = N_\psi^\pm / L$ are the Ψ up and down mover densities, N_ψ^+, N_ψ^- standing for the number of Ψ particle moving in the $+z$ or $-z$ directions, respectively. Note that the total number of particles of this kind is thus $N_\psi = N_\psi^+ + N_\psi^- + 1$ since there is the additional rest state obtained for $k=0$. After some algebra in Eq. (74), using Eq. (84), the parameters, for the Ψ field, read

$$E_\psi = \frac{\bar{m}^2}{4\pi}\{\tilde{\rho}_\psi^{+2} - \tilde{\rho}_\psi^{-2} + [\tilde{\rho}_\psi^+ \sqrt{1+\tilde{\rho}_\psi^{+2}} + \tilde{\rho}_\psi^- \sqrt{1+\tilde{\rho}_\psi^{-2}}] + \ln[(\sqrt{1+\tilde{\rho}_\psi^{+2}} + \tilde{\rho}_\psi^+)(\sqrt{1+\tilde{\rho}_\psi^{-2}} + \tilde{\rho}_\psi^-)]\} + (\tilde{\rho}_\psi^\pm \leftrightarrow \bar{\tilde{\rho}}_\psi^\pm), \tag{85}$$

$$P_\psi = \frac{\bar{m}^2}{4\pi}\{\tilde{\rho}_\psi^{+2} - \tilde{\rho}_\psi^{-2} + [\tilde{\rho}_\psi^+ \sqrt{1+\tilde{\rho}_\psi^{+2}} + \tilde{\rho}_\psi^- \sqrt{1+\tilde{\rho}_\psi^{-2}}] - \ln[(\sqrt{1+\tilde{\rho}_\psi^{+2}} + \tilde{\rho}_\psi^+)(\sqrt{1+\tilde{\rho}_\psi^{-2}} + \tilde{\rho}_\psi^-)]\} + (\tilde{\rho}_\psi^\pm \leftrightarrow \bar{\tilde{\rho}}_\psi^\pm), \tag{86}$$

where $\tilde{\rho}_\psi$ stands for the dimensionless Ψ mover density

$$\tilde{\rho}_\psi = \frac{2\pi}{\bar{m}} \rho_\psi, \tag{87}$$

while $\bar{\tilde{\rho}}_\psi$ is defined in the same way for the Ψ antiparticle states. Similarly, the two other parameters $\bar{E}_\psi$ and $\bar{P}_\psi$ read

$$\bar{E}_\psi = \frac{\bar{m}^2}{4\pi}\{-\tilde{\rho}_\psi^{+2} + \tilde{\rho}_\psi^{-2} + [\tilde{\rho}_\psi^+ \sqrt{1+\tilde{\rho}_\psi^{+2}} + \tilde{\rho}_\psi^- \sqrt{1+\tilde{\rho}_\psi^{-2}}] + \ln[(\sqrt{1+\tilde{\rho}_\psi^{+2}} + \tilde{\rho}_\psi^+)(\sqrt{1+\tilde{\rho}_\psi^{-2}} + \tilde{\rho}_\psi^-)]\} + (\tilde{\rho}_\psi^\pm \leftrightarrow \bar{\tilde{\rho}}_\psi^\pm), \tag{88}$$

$$\bar{P}_\psi = \frac{\bar{m}^2}{4\pi}\{\tilde{\rho}_\psi^{+2} - \tilde{\rho}_\psi^{-2} - [\tilde{\rho}_\psi^+ \sqrt{1+\tilde{\rho}_\psi^{+2}} + \tilde{\rho}_\psi^- \sqrt{1+\tilde{\rho}_\psi^{-2}}] + \ln[(\sqrt{1+\tilde{\rho}_\psi^{+2}} + \tilde{\rho}_\psi^+)(\sqrt{1+\tilde{\rho}_\psi^{-2}} + \tilde{\rho}_\psi^-)]\} + (\tilde{\rho}_\psi^\pm \leftrightarrow \bar{\tilde{\rho}}_\psi^\pm). \tag{89}$$

Note that these parameters depend differently on the up and down mover densities as expected for chiral coupling of the fermions to the string forming Higgs field. Recall that in the massless case the zero modes associated with the Ψ and $\mathcal{X}$ fields can only propagate in the $-z$ and $+z$ direction, respectively [8,25,28]. The same relationships also hold for the $\mathcal{X}$ field by using the relevant dimensionless mover densities $\tilde{\rho}_\chi^\pm$ and $\bar{\tilde{\rho}}_\chi^\pm$. Although the equation of state can be derived as a function of these four parameters for each fermion field $\mathcal{F}$, it is convenient at this stage to perform some physical simplifications. Contrary to the zero mode case, the coupling between massive particles and antiparticles of the same species $\mathcal{F}$ does not vanish along the string. As a result, it is reasonable to consider that the only kind surviving at zero temperature corresponds to the one which was in excess in the plasma in which the string was formed during the phase transition. On the other hand, the energetically favored distribution at zero temperature involves necessarily the same number of $\mathcal{F}$ up and down movers, each filling the accessible states living on each branch of the mass hyperbola (see Fig. 9). As a result, in the considered energy scale, it seems reasonable to consider only one state parameter per mass instead of the four initially introduced by quantization, namely $\tilde{\rho}_\mathcal{F} = \tilde{\rho}_\mathcal{F}^+ = \tilde{\rho}_\mathcal{F}^-$, for a plasma dominated by particles, say.

Setting these simplifications in Eqs. (85)–(89), by means of Eqs. (81) and (82) the energy density and the tension associated with the lowest massive modes now read

$$U = M^2 + \frac{1}{2\pi} \sum_\mathcal{F} \bar{m}_\mathcal{F}^2 \ln[\sqrt{1+\tilde{\rho}_\mathcal{F}^2} + \tilde{\rho}_\mathcal{F}] + \frac{1}{\pi}\left[\sum_\mathcal{F} \bar{m}_\mathcal{F}^2 ||\Sigma_{\mathrm{Y}\mathcal{F}}^2|| \tilde{\rho}_\mathcal{F} \sqrt{1+\tilde{\rho}_\mathcal{F}^2} \times \sum_\mathcal{F} \bar{m}_\mathcal{F}^2 ||\Sigma_{\mathrm{X}\mathcal{F}}^2|| \tilde{\rho}_\mathcal{F} \sqrt{1+\tilde{\rho}_\mathcal{F}^2}\right]^{1/2}, \tag{90}$$

$$T = M^2 + \frac{1}{2\pi} \sum_\mathcal{F} \bar{m}_\mathcal{F}^2 \ln[\sqrt{1+\tilde{\rho}_\mathcal{F}^2} + \tilde{\rho}_\mathcal{F}] - \frac{1}{\pi}\left[\sum_\mathcal{F} \bar{m}_\mathcal{F}^2 ||\Sigma_{\mathrm{Y}\mathcal{F}}^2|| \tilde{\rho}_\mathcal{F} \sqrt{1+\tilde{\rho}_\mathcal{F}^2} \times \sum_\mathcal{F} \bar{m}_\mathcal{F}^2 ||\Sigma_{\mathrm{X}\mathcal{F}}^2|| \tilde{\rho}_\mathcal{F} \sqrt{1+\tilde{\rho}_\mathcal{F}^2}\right]^{1/2}. \tag{91}$$

The sum runs over the two lowest massive bound states, each one being associated to the two fermion fields trapped in the vortex, namely Ψ and $\mathcal{X}$, and have $\bar{m}_\psi$ and $\bar{m}_\chi$ masses, respectively. As a result, the equation of state involves two independent parameters, $\tilde{\rho}_\psi$ and $\tilde{\rho}_\chi$, in the zero-temperature and infinite string limit. The energy per unit length and the tension have been plotted in Fig. 10, for the lowest massive modes in the nonperturbative sector. The curves are essentially the same in the perturbative sector, but the variations around the Goto-Nambu case $U=T=M^2$ are much more damped. For reasonable values of the transverse normalizations, e.g., $||\Sigma_{\mathrm{X}}^2|| \sim ||\Sigma_{\mathrm{Y}}^2|| \sim 0.5$, and for small values of the dimensionless parameters $\tilde{\rho}_\psi$ and $\tilde{\rho}_\chi$, the energy density is

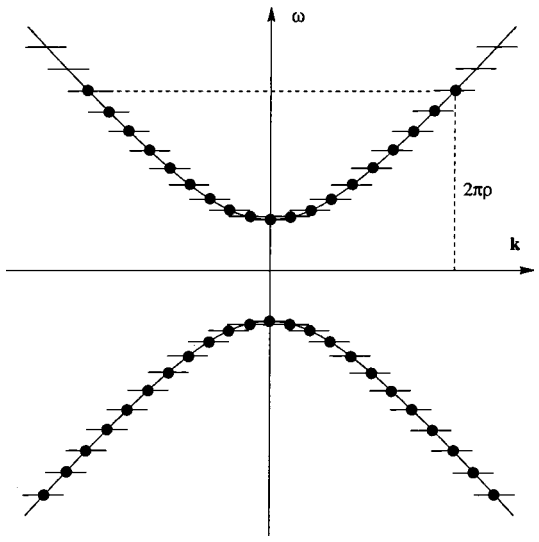

FIG. 9. The filling of massive states trapped in the string, as expected in the zero-temperature limit, for a particular mass and for one species, Ψ or $\mathcal{X}$ say. All antiparticles have disappeared by annihilation with particles during cooling, and the interactions between particles moving in opposite directions, as their coupling to the gauge field, lead to the energetically favored configuration with same number of up and down movers. Obviously, the Fermi level is necessarily below the vacuum mass of the relevant fermion.

found to grow linearly with $\tilde{\rho}_\psi$ and $\tilde{\rho}_\chi$, whereas the tension varies quadratically. As can be seen in Eq. (90), due to the minus sign in T, all linear terms in $\tilde{\rho}$ vanish near origin, whereas it is not the case for the energy density. However, for higher values of the densities, the quadratic terms dominate and both energy density and tension end up being quadratic functions of $\tilde{\rho}$. On the other hand, according to the macroscopic formalism [14], the string becomes unstable with respect to transverse perturbations when the tension takes on negative values, as in Fig. 10 for high densities. Moreover, the decrease of the tension is more damped in the perturbative sector, and the negative values cannot actually be reached for acceptable values of $\tilde{\rho}$, i.e., $\tilde{\rho}<m_{\rm f}/\overline{m}$. As a result, the rapid decrease of the tension with respect to the fermion densities constrains the nonperturbative sector where the string is able to carry massive fermionic currents. For each mass, the higher acceptable value of the $\tilde{\rho}$ ensuring transverse normalizability is roughly $m_{\rm f}/\overline{m}$, and from Eq. (90), the tension becomes negative at this density for $m_{\rm f}^2 \sim 4\pi M^2$. Much higher values of $m_{\rm f}$ will thus yield to empty massive states.

As previously noted, the energy density and tension for massive modes no longer verify the fixed trace equation of state found with the zero modes alone. As a result, the longitudinal perturbation propagation speed $c_{\rm L}^2=-dT/dU$ is no longer equal to the speed of light, and it is even no longer well defined since the equation of state involves more than one state parameter. A necessary condition for longitudinal stability can nevertheless be stated by verifying that all the perturbation propagation speeds $-(\partial T/\partial\tilde{\rho})/(\partial U/\partial\tilde{\rho})$ obtained from variation of only one state parameter are positive and less than the speed of light. The longitudinal and transverse perturbation propagation speeds, $c_{\rm L}^2$ and $c_{\rm T}^2=T/U$, respectively, have been plotted in Fig. 11 in the case where there is only one species trapped as massive mode, Ψ or $\mathcal{X}$ say. It is interesting to note that there is a transition between a supersonic regime obtained at low fermion density, and a subsonic at high fermion density. Moreover, the transition density between the two regimes is all the more so high as the coupling constant $m_{\rm f}/m_{\rm h}$ is weak. It is not surprising to recover such zero-mode-like subsonic behavior [25,33] for densities much higher than the rest mass, since in these cases the ultrarelativistic limit applies. On the other hand, since the mass of the massive mode decreases with the coupling constant as in Fig. 5, the transition will occur earlier in the nonperturbative sector, as can be seen in Fig. 12. Note that the subsonic region is also limited by the maximum allowed values of the massive fermion densities, i.e, $\sim m_{\rm f}/\overline{m}$, and the regions of transverse instabilities where $c_{\rm T}^2$ becomes negative. Inclusion of the other species does not change signifi-

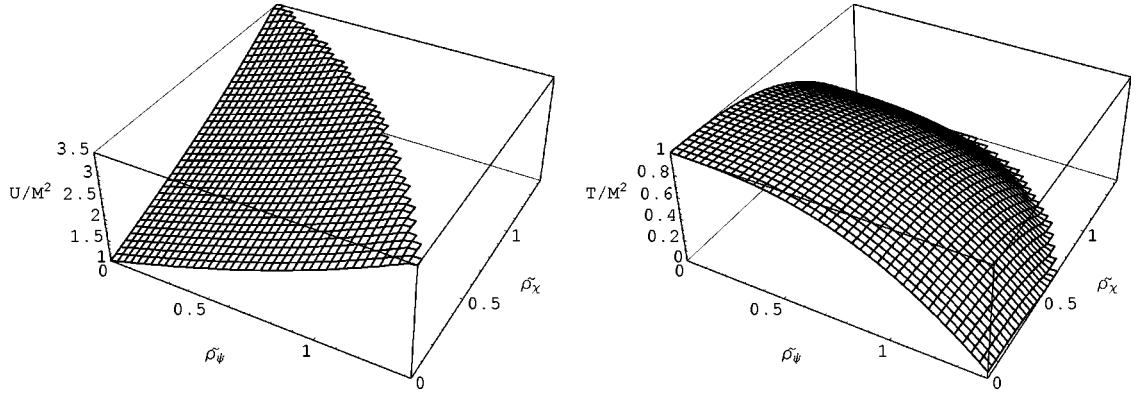

FIG. 10. The energy per unit length and the tension, in unit of M^2, for the lowest massive modes alone, plotted as function of the dimensionless effective densities of the two fermion fields, $\tilde{\rho}_\psi$ and $\tilde{\rho}_\chi$. The parameters have been chosen in the nonperturbative sector, with $m_{\rm f}/m_{\rm h}\sim 3$ and $\overline{m}_\chi\sim\overline{m}_\psi\sim 0.6m_{\rm f}$. Note the linear variation of the energy density near the origin whereas the tension varies quadratically. Moreover, in the allowed range for fermion densities, i.e., less than the fermion vacuum mass, the tension vanishes and the string becomes unstable with respect to transverse perturbations.

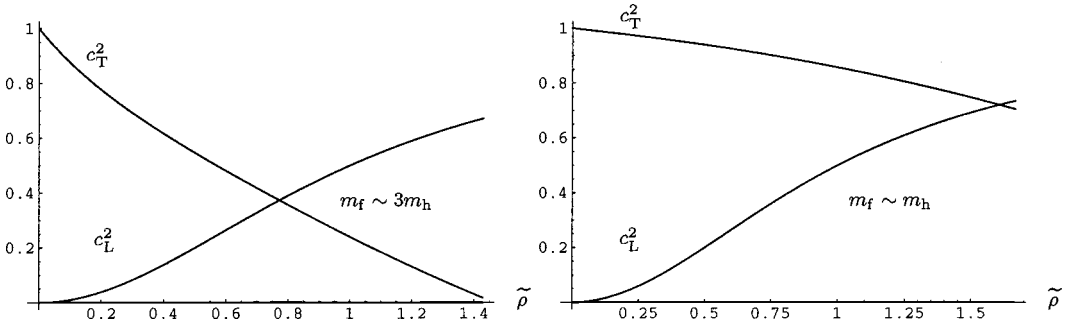

FIG. 11. The squared longitudinal and transverse perturbations propagation speeds for one massive species only, plotted as functions of the dimensionless fermion density $\tilde{\rho}$, for two values of the coupling constant m_f/m_h. Note the transition between subsonic and supersonic behaviors takes place at a cross density, $\tilde{\rho}_\times$ say, which decreases with the coupling constant (see Fig. 12).

cantly these behaviors, the main effect being to lower c_T^2 with respect to the other fermion density, as can be seen in Fig. 10.

The current magnitude can also be derived from the averaged current operators in the zero temperature and infinite string limit. From Eq. (76), using Eqs. (39) and (61), once the transverse coordinates have been integrated over, the world sheet components read

$$\langle \overline{j^0} \rangle = -\sum_{\mathcal{F}} \frac{\overline{m}_{\mathcal{F}}}{\pi} (qc_{\mathcal{F}_R} ||\overline{\alpha_1^2} + \overline{\alpha_2^2}|| + qc_{\mathcal{F}_L} ||\overline{\alpha_4^2} + \overline{\alpha_3^2}||)\tilde{\rho}_{\mathcal{F}},$$
$$\langle \overline{j^3} \rangle = -\sum_{\mathcal{F}} \frac{\overline{m}_{\mathcal{F}}}{\pi} (qc_{\mathcal{F}_R} ||\overline{\alpha_1^2} - \overline{\alpha_2^2}|| + qc_{\mathcal{F}_L} ||\overline{\alpha_4^2} - \overline{\alpha_3^2}||)\tilde{\rho}_{\mathcal{F}}. \tag{92}$$

The current magnitude $\mathcal{C}^2 = \langle \overline{j^0} \rangle^2 - \langle \overline{j^3} \rangle^2$ therefore reads

$$\mathcal{C}^2 = 4\left(\sum_{\mathcal{F}} \frac{\overline{m}_{\mathcal{F}}}{\pi} F_{Y\mathcal{F}} \tilde{\rho}_{\mathcal{F}} \right)\left(\sum_{\mathcal{F}} \frac{\overline{m}_{\mathcal{F}}}{\pi} F_{X\mathcal{F}} \tilde{\rho}_{\mathcal{F}} \right), \tag{93}$$

where $F_{X\mathcal{F}}$ and $F_{Y\mathcal{F}}$ denote the transverse effective charges

$$F_{Y\mathcal{F}} = qc_{\mathcal{F}_R} ||\overline{\alpha_1^2}|| + qc_{\mathcal{F}_L} ||\overline{\alpha_4^2}||,$$
$$F_{X\mathcal{F}} = qc_{\mathcal{F}_R} ||\overline{\alpha_2^2}|| + qc_{\mathcal{F}_L} ||\overline{\alpha_3^2}||, \tag{94}$$

already introduced for the zero mode currents [25]. In the case of one massive species only, the charge current magnitude simplifies to

$$\mathcal{C}^2 = 4\frac{\overline{m}^2}{\pi^2} F_X F_Y \tilde{\rho}^2, \tag{95}$$

and thus the sign of $\mathcal{C}^2$ is only given by the sign of $F_X F_Y$, which is generally positive for reasonable values of the transverse normalizations, e.g., $||\Sigma_X^2|| \sim ||\Sigma_Y^2|| \sim 0.5$. As a result, the charge current generated by only one massive species is always timelike [26], contrary to the zero mode charge current which was found to be possibly timelike, but also spacelike [25], owing to the allowed exitations of antiparticle zero mode states. As noted above, the antiparticle states cannot exist for massive modes due to the nonvanishing cross section along the string between massive particles and antiparticles. Moreover, and as it was the case for the zero modes, unless there is only one massive species trapped in the string, the magnitude of the charge current is not a sufficient state parameter, contrary to the bosonic current-carrier case [15].

B. General case

From the numerical approach in Sec. III B 4, as soon as the nonperturbative sectors are considered, additional massive bound states become relevant, and it is reasonable to consider that, in the zero-temperature limit, all these accessible massive states will be also be filled. Moreover, the complete description of the string state also requires the inclusion of the zero modes in addition to the massive ones.

1. Full stress tensor

The effective two-dimensional energy momentum tensor, involving all trapped modes in the cosmic string, can be obtained from Eq. (80) by replacing the sum over the two lowest massive modes with the sum over all the accessible masses, plus the zero mode terms previously derived in Ref. [25]. In the preferred frame where the stress tensor is diagonal, after some algebra, the energy density and tension therefore read

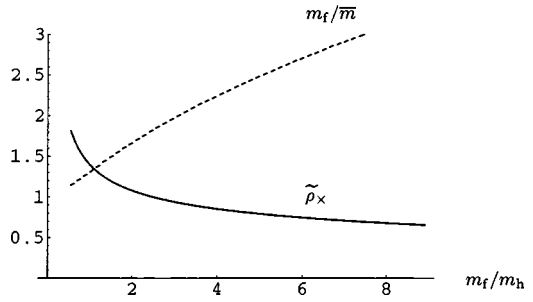

FIG. 12. The cross dimensionless density $\tilde{\rho}_\times$, i.e., the dimensionless fermion density for which the transverse and longitudinal perturbation propagation speeds are equal, plotted as function of the coupling constant m_f/m_h, for one massive species only. The dashed curve shows the maximum allowed values $m_f/\overline{m}$ of the massive fermion density ensuring transverse normalizability. The transition from supersonic regime to subsonic can thus occurs only in the nonperturbative sector, below this frontier.

$$U=M^2+\frac{1}{2\pi}\sum_{\mathcal{F},l}\overline{m}^2_{\mathcal{F}_l}\ln\Big[\sqrt{1+\tilde{\rho}^2_{\mathcal{F}_l}}+\tilde{\rho}_{\mathcal{F}_l}\Big]+\frac{1}{\pi}\Bigg[\Bigg(4\pi^2\mathcal{R}^2_\chi+\sum_{\mathcal{F},l}\overline{m}^2_{\mathcal{F}_l}||\Sigma^2_{\mathrm{Y}\mathcal{F}_l}||\tilde{\rho}_{\mathcal{F}_l}\sqrt{1+\tilde{\rho}^2_{\mathcal{F}_l}}\Bigg)\Bigg(4\pi^2\mathcal{R}^2_\psi+\sum_{\mathcal{F},l}\overline{m}^2_{\mathcal{F}_l}||\Sigma^2_{\mathrm{X}\mathcal{F}_l}||\tilde{\rho}_{\mathcal{F}_l}\sqrt{1+\tilde{\rho}^2_{\mathcal{F}_l}}\Bigg)\Bigg]^{1/2}, \tag{96}$$

$$T=M^2+\frac{1}{2\pi}\sum_{\mathcal{F},l}\overline{m}^2_{\mathcal{F}_l}\ln\Big[\sqrt{1+\tilde{\rho}^2_{\mathcal{F}_l}}+\tilde{\rho}_{\mathcal{F}}\Big]-\frac{1}{\pi}\Bigg[\Bigg(4\pi^2\mathcal{R}^2_\chi+\sum_{\mathcal{F},l}\overline{m}^2_{\mathcal{F}_l}||\Sigma^2_{\mathrm{Y}\mathcal{F}_l}||\tilde{\rho}_{\mathcal{F}_l}\sqrt{1+\tilde{\rho}^2_{\mathcal{F}_l}}\Bigg)\Bigg(4\pi^2\mathcal{R}^2_\psi+\sum_{\mathcal{F},l}\overline{m}^2_{\mathcal{F}_l}||\Sigma^2_{\mathrm{X}\mathcal{F}_l}||\tilde{\rho}_{\mathcal{F}_l}\sqrt{1+\tilde{\rho}^2_{\mathcal{F}_l}}\Bigg)\Bigg]^{1/2}. \tag{97}$$

The sums run over all accessible massive bound states l with masses $\overline{m}_{\mathcal{F}_l}$ of each fermion $\mathcal{F}$, i.e., Ψ and $\mathcal{X}$. The additional parameters $\mathcal{R}_\chi$ and $\mathcal{R}_\psi$ are the particle densities trapped in the string in the form of zero modes, for the $\mathcal{X}$ and Ψ field, respectively, with same notation as in Ref. [25]. Note that the zero mode contribution can also be obtained from the null mass limit in Eq. (90). As a result, the full expression of energy per unit length and tension seems to involve as many state parameters as trapped modes in the string.

2. Equation of state

As for the lowest massive modes, it is convenient to perform some approximations owing to the energetically favored filling of the involved states, in the zero-temperature limit. In particular, it is reasonable to consider that the nonvanishing cross sections between massive modes, and between zero modes and massive modes, lead to the filling of all the accessible states with energy lower than a Fermi energy, $\mathcal{E}_\mathcal{F}$ say, for each fermion field $\mathcal{F}$. As a result, the energetically favored filling takes place by successive jumps from the lower masses to the highest ones, until the last mass hyperbola with $\overline{m}_{\mathcal{F}_l}\sim\mathcal{E}_\mathcal{F}$ is reached. Obviously, this filling begins with the zero modes, next with the lowest massive modes and so on. On the other hand, only the particle states are assumed to be relevant because of the assumed annihilation of the antiparticle states, as discussed in Sec. V A 2. As a result, the Fermi levels, $\nu_\mathcal{F}$ say, can be defined through the zero modes filling only, as the line densities of zero mode exitations trapped in the string (see Fig. 13), and thus play the role of state parameters.

According to the so-defined state parameters the massive exitation densities, $\rho_{\mathcal{F}_l}$, in Eqs. (96) and (97), reduce to

$$\rho_{\mathcal{F}_l}=\Big(\nu_\mathcal{F}-\frac{\overline{m}_{\mathcal{F}_l}}{2\pi}\Big)\Theta\Big[\nu_\mathcal{F}-\frac{\overline{m}_{\mathcal{F}_l}}{2\pi}\Big], \tag{98}$$

with Θ function is the Heavyside step function, as expected for energy scales less than the rest mass of the considered massive mode. The zero mode density simply reads

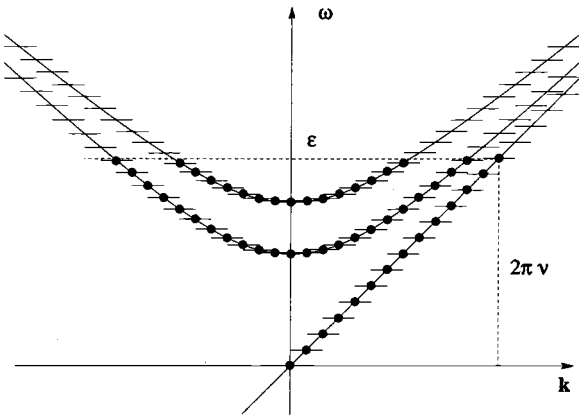

FIG. 13. The accessible states, for the $\mathcal{X}$ fermions, in the zero-temperature limit. The zero modes are represented by the chiral line $\omega=k$, while the massive modes appear as mass hyperbolae. The Fermi levels are therefore dependent of the considered energy scale $\mathcal{E}$, since the filling is performed by successive jumps from the zero-modes to the massive ones, with $\overline{m}_l\sim\mathcal{E}$. As a result, under these approximations, each trapped species leads to only one state parameter which can be identified with the Fermi level of the zero mode exitations, namely $\nu=\mathcal{E}/2\pi$. Note that the antiparticle states have not been represented due to their assumed annihilation.

$$\mathcal{R}_\mathcal{F}=\nu_\mathcal{F} \tag{99}$$

for zero mode particle states alone. From Eqs. (98) and (99), and the definition of the dimensionless densities in Eq. (87),

$$\tilde{\rho}_{\mathcal{F}_l}=\frac{2\pi}{\overline{m}_{\mathcal{F}_l}}\rho_{\mathcal{F}_l}, \tag{100}$$

the energy per unit length and the tension now depend explicitly of the two state parameters only, namely ν_ψ and ν_χ. By means of Eq. (96), the energy density reads

$$U=M^2+\frac{1}{2\pi}\sum_{\overline{m}_{\mathcal{F}_l}\leqslant 2\pi\nu_\mathcal{F}}\overline{m}^2_{\mathcal{F}_l}\ln\Bigg[\sqrt{1+\Big(\frac{2\pi}{\overline{m}_{\mathcal{F}_l}}\nu_\mathcal{F}-1\Big)^2}+\frac{2\pi}{\overline{m}_{\mathcal{F}_l}}\nu_\mathcal{F}-1\Bigg]+\frac{1}{\pi}\Bigg[(2\pi\nu_\chi)^2+\sum_{\overline{m}_{\mathcal{F}_l}\leqslant 2\pi\nu_\mathcal{F}}\overline{m}^2_{\mathcal{F}_l}||\Sigma^2_{\mathrm{Y}\mathcal{F}_l}||\times\Big(\frac{2\pi}{\overline{m}_{\mathcal{F}_l}}\nu_\mathcal{F}-1\Big)\sqrt{1+\Big(\frac{2\pi}{\overline{m}_{\mathcal{F}_l}}\nu_\mathcal{F}-1\Big)^2}\Bigg]^{1/2}\times\Bigg[(2\pi\nu_\psi)^2+\sum_{\overline{m}_{\mathcal{F}_l}\leqslant 2\pi\nu_\mathcal{F}}\overline{m}^2_{\mathcal{F}_l}||\Sigma^2_{\mathrm{X}\mathcal{F}_l}||\times\Big(\frac{2\pi}{\overline{m}_{\mathcal{F}_l}}\nu_\mathcal{F}-1\Big)\sqrt{1+\Big(\frac{2\pi}{\overline{m}_{\mathcal{F}_l}}\nu_\mathcal{F}-1\Big)^2}\Bigg]^{1/2}, \tag{101}$$

while the tension is obtained from Eq. (97)

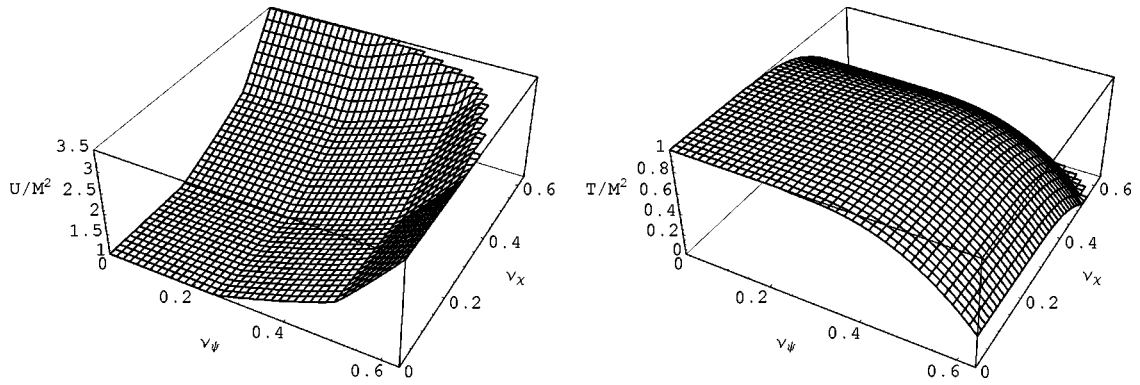

FIG. 14. The energy per unit length and the tension plotted as function of the two state parameters, i.e., the zero mode densities, in the nonperturbative sector $m_{\rm f}/m_{\rm h}\sim 4$. Two additional massive bound states have been considered with respective masses $\overline{m}/m_{\rm f}\sim 0.4$ and $\overline{m}/m_{\rm f}\sim 0.6$. In the zero-temperature limit, the filling of the accessible states is performed by successive jumps as soon as the Fermi level reaches one mass hyperbola (see Fig. 13). As a result, for the lowest values of the state parameters, only the zero modes are relevant and the fixed trace equation of state, $U+T=2M^2$, is verified, then the first and second massive modes are successively reached and become rapidly dominant. As can be seen near the origin, the smooth variations induced by the zero modes appear completely negligible compared to the massive ones. In the perturbative sectors, these behaviors are essentially the same, but the induced variations of the density energy and the tension are all the more small.

$$
\begin{aligned}
T = M^2 + \frac{1}{2\pi} \sum_{\overline{m}_{\mathcal{F}_l} \leqslant 2\pi\nu_{\mathcal{F}}} \overline{m}_{\mathcal{F}_l}^2 \ln\Bigg[& \sqrt{1+\left(\frac{2\pi}{\overline{m}_{\mathcal{F}_l}}\nu_{\mathcal{F}}-1\right)^2} \\
& + \frac{2\pi}{\overline{m}_{\mathcal{F}_l}}\nu_{\mathcal{F}}-1 \Bigg] - \frac{1}{\pi}\Bigg[(2\pi\nu_\chi)^2 + \sum_{\overline{m}_{\mathcal{F}_l} \leqslant 2\pi\nu_{\mathcal{F}}} \overline{m}_{\mathcal{F}_l}^2 ||\Sigma^2_{\mathrm{Y}\mathcal{F}_l}|| \\
& \times \left(\frac{2\pi}{\overline{m}_{\mathcal{F}_l}}\nu_{\mathcal{F}}-1\right) \sqrt{1+\left(\frac{2\pi}{\overline{m}_{\mathcal{F}_l}}\nu_{\mathcal{F}}-1\right)^2} \Bigg]^{1/2} \\
& \times \Bigg[(2\pi\nu_\psi)^2 + \sum_{\overline{m}_{\mathcal{F}_l} \leqslant 2\pi\nu_{\mathcal{F}}} \overline{m}_{\mathcal{F}_l}^2 ||\Sigma^2_{\mathrm{X}\mathcal{F}_l}|| \\
& \times \left(\frac{2\pi}{\overline{m}_{\mathcal{F}_l}}\nu_{\mathcal{F}}-1\right) \sqrt{1+\left(\frac{2\pi}{\overline{m}_{\mathcal{F}_l}}\nu_{\mathcal{F}}-1\right)^2} \Bigg]^{1/2}. \qquad (102)
\end{aligned}
$$

The full energy per unit length and tension have been plotted in Fig. 14 for a configuration including two massive bound states, in addition to the zero mode ones. Due to the zero-temperature limit, for densities smaller than the first accessible mass, the Heavyside functions in Eq. (98) vanish, as a result, from Eqs. (101) and (102) the fixed trace equation of state is recovered [25] with

$$U = M^2 + 4\pi\nu_\chi\nu_\psi, \quad T = M^2 - 4\pi\nu_\chi\nu_\psi. \qquad (103)$$

Once the first mass hyperbola is reached, the behaviors of the energy per unit length and tension are clearly modified and become very rapidly dominated by the mass terms, and, as found for the lowest massive modes alone, the energy density begins to grow linearly with respect to the state parameters, whereas the tension decreases quadratically. Actually, the plotted curves in Fig. 14 show slope discontinuities each time the phase space is enlarged due to the income of accessible massive bound states (see Fig. 13).

On the other hand, it is reasonable to expect competition between the subsonic regimes induced by zero mode currents, or ultrarelativistic massive modes, and the supersonic ones coming from massive currents. In all cases, when the state parameters remain small, only the chiral massless states are accessible and the regime is obviously subsonic, as can be seen in Fig. 15. However, the massive mode filling modifies radically this behavior, and as found for the lowest massive modes alone, as soon as a mass hyperbola is reached, the longitudinal perturbations propagation speed falls drastically and ends up being less than the transverse perturbation velocity. There is a rapid transition from the subsonic to the supersonic regime. For higher densities ν, the behavior depends on the coupling constant. More precisely, in the nonperturbative sector, the ultrarelativistic limit can be applied before the energy scales reach the fermion vacuum masses, and thus the subsonic regime is recovered, whereas it is not the case in the perturbative sector, as can be seen in Fig. 15.

3. Discussion

All these results have been derived without considering the back reaction effects induced by the trapped charge currents along the string [see Eq. (92)]. As was already discussed for the zero modes in Ref. [25], these currents yield back reacted gauge field, B_t and B_z, which might modify the vortex background and the fermionic equations of motion. However, such perturbations of the Higgs and orthoradial gauge field profiles (see Fig. 1) can be neglected for B_tB^t and B_zB^z small compared to the string forming gauge field $B_\theta B^\theta \sim m_{\rm b}^2$. Using Eqs. (40) and (92), the dimensionless charge currents associated with one massive bound state, and generating the dimensionless gauge fields $B_\alpha/m_{\rm b}$, roughly read

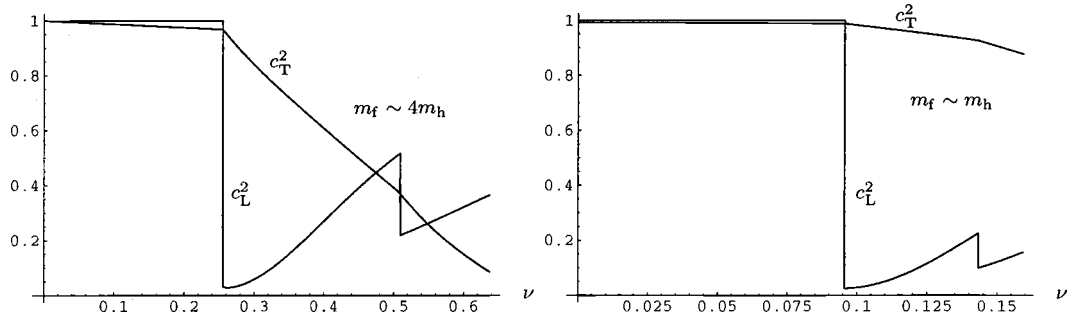

FIG. 15. The squared longitudinal and transverse perturbation propagation speeds for a spectrum involving two massive states in addition to the zero mode, plotted as functions of the state parameter $\nu_{\mathcal{F}}$ of one species, the other being fixed to a particular value. The curves have been plotted for two values of the coupling constant to the Higgs field, $m_f/m_h \sim 1$ and $m_f/m_h \sim 4$. Note the successive transitions between subsonic and supersonic behaviors according to the allowed jumps to the mass hyperbolae. However, the fermion vacuum mass limit does not allow the ultrarelativistic limit to take place in the perturbative sector, as it was the case for the lowest massive modes alone. In this case, the string dynamics follows a supersonic regime as soon as the first massive bound state is filled.

$$\tilde{j}^{\alpha} \sim \frac{c_{\mathcal{F}}}{c_{\phi}} \tilde{\rho}_{\mathcal{F}} \frac{\bar{m}_{\mathcal{F}}}{2\pi^2 \eta}, \tag{104}$$

with $c_{\mathcal{F}}$ the fermion charges, i.e., $c_{\mathcal{F}_R}$ or $c_{\mathcal{F}_L}$. As a result, the back reaction on the vortex background is negligible as long as $\bar{m} < 2\pi^2 \eta$, which is clearly satisfied in the full perturbative sector. Moreover, since $m_h = \eta\sqrt{\lambda}$, the previous derivations of the equation of state are also valid in the nonperturbative sector provided $\bar{m} < 2\pi^2 m_h/\sqrt{\lambda}$, and thus depend on the values of self-coupling constant of the Higgs field λ, but also on the mass spectrum. As can be seen in Fig. 5, the ratio $\bar{m}/m_f$ decreases with the fermion vacuum mass m_f, as a result $\bar{m}/m_h$ increases all the more slowly, which allows to have both $m_f > m_h$ and $\bar{m} < 2\pi^2 m_h/\sqrt{\lambda}$.

Moreover, in order for the new gauge fields B_t and B_z to not significantly modify the fermionic equations of motion, from Eq. (13), they have to verify $q c_{\phi} B_{\alpha} < \omega \sim \bar{m}_{\mathcal{F}}$. As a result, Eq. (104), and $B_{\alpha}/m_b \sim \tilde{j}^{\alpha}$ yield the condition

$$\frac{m_b^2}{\eta^2} \frac{c_{\mathcal{F}}}{c_{\phi}} < 1. \tag{105}$$

As expected, it is essentially the same condition as the one previously derived for the zero modes alone [25]. On the other hand, although the back reaction on the fermionic equations of motion can deeply modify the zero mode currents [34], since the massive bound states are no longer eigenstates of the $\gamma^0\gamma^3$ operator, it is reasonable to assume that rather than modify their nature and existence significantly, the back reaction gauge fields may only modify their mass spectrum. In this sense, back reaction would indeed be a correction.

VI. CONCLUSION

The relevant characteristic features of Dirac fermions trapped in a cosmic string in the form of massive bound states have been study numerically, in the framework of the Witten model, and in the neutral limit. By means of a two-dimensional quantization of the associated spinor fields along the string world sheet, the energy per unit length and the tension of a cosmic string carrying any kind of fermionic current, massive or massless, have been computed, and found to involve as many state parameters as different trapped modes. However, in the zero-temperature limit, only two have been found to be relevant and they can be defined as the density numbers of the chiral zero mode exitations associated with the two fermions Ψ and $\mathcal{X}$ coupled to the Higgs field.

As a result, it was shown that the fixed trace equation of state no longer applies as soon as massive states are filled, i.e., for energy scales larger than the lowest massive mode belonging to the mass spectrum. Moreover, the filling of massive states leads to a rapid transition from the subsonic regime, relevant with massless, or ultrarelativistic currents, to supersonic. Such properties could be relevant in vorton evolution since it has been shown that supersonic regimes generally lead to their classical instabilities [21]. As a result, in the perturbative sectors for which $m_f < m_h$, the protovortons could be essentially produced at energy scales necessarily smaller than the lower mass of the spectrum, where the fermionic currents consist essentially in zero modes. In this way, vortons with fermionic currents could be included in the more general two energy scale models [11]. However, the present conclusions are restricted to parameter domains of the model where the back reaction can be neglected. Although it is reasonable to consider that the back reaction effects may simply modify the massive bound states through their mass values, their influence on zero modes are expected to be much more significant. In particular, the modified zero modes cannot be any longer eigenstates of the $\gamma^0\gamma^3$ operator [25], so one may conjecture that they acquire an effective mass, leading to massive states potentially instable for cosmic string loops.

ACKNOWLEDGMENTS

It is a pleasure to thank particularly P. Peter for many fruitful and helpfull discussions. I also wish to acknowledge M. Lemoine, J. Martin, and O. Poujade for advice and various enlightening discussions.

[1] T.W.B. Kibble, Phys. Rep. **67**, 183 (1980).
[2] D.P. Bennett, F.R. Bouchet, and A. Stebbins, Nature (London) **335**, 410 (1988); D.P. Bennett and F.R. Bouchet, Phys. Rev. D **41**, 2408 (1990); L. Perivolaropoulos, Astrophys. J. **451**, 429 (1995); B. Allen, R.R. Caldwell, S. Dodelson, L. Knox, E.P.S. Shellard, and A. Stebbins, Phys. Rev. Lett. **79**, 2624 (1997).
[3] P.P. Avelino, E.P.S. Shellard, J.H.P. Wu, and B. Allen, Phys. Rev. D **60**, 023511 (1999); J.H.P. Wu, P.P. Avelino, E.P.S. Shellard, and B. Allen, astro-ph/9812156; C. Contaldi, M. Hindmarsh, and J. Magueijo, Phys. Rev. Lett. **82**, 679 (1999).
[4] F.R. Bouchet, P. Peter, A. Riazuelo, and M. Sakellariadou, Phys. Rev. D (to be published), astro-ph/0005022.
[5] Y.B. Zel'dovich, Mon. Not. R. Astron. Soc. **192**, 663 (1980).
[6] A. Vilenkin, Phys. Rev. Lett. **46**, 1169 (1981); **46**, 1496(E) (1981).
[7] P. de Bernardis *et al.*, Nature (London) **404**, 955 (2000); P. de Bernardis *et al.*, astro-ph/0105296.
[8] E. Witten, Nucl. Phys. **B249**, 557 (1985).
[9] J.P. Ostriker, C. Thompson, and E. Witten, Phys. Lett. B **180**, 231 (1986).
[10] R.L. Davis, Phys. Rev. D **38**, 3722 (1988).
[11] R. Brandenberger, B. Carter, A.C. Davis, and M. Trodden, Phys. Rev. D **54**, 6059 (1996).
[12] R.L. Davis, Phys. Rev. D **36**, 2267 (1987); C.T. Hill and L.M. Widrow, Phys. Lett. B **189**, 17 (1987); M. Hindmarsh, *ibid.* **200**, 429 (1988).
[13] A.E. Everett, Phys. Rev. Lett. **61**, 1807 (1988); J. Ambjørn, N.K. Nielsen, and P. Olesen, Nucl. Phys. **B310**, 625 (1988).
[14] B. Carter, Phys. Lett. B **224**, 61 (1989); **228**, 466 (1989); Nucl. Phys. **B412**, 345 (1994); B. Carter, P. Peter, and A. Gangui, Phys. Rev. D **55**, 4647 (1997); A. Gangui, P. Peter, and C. Boehm, *ibid.* **57**, 2580 (1998).
[15] P. Peter, Phys. Rev. D **45**, 1091 (1992).
[16] P. Peter, Phys. Rev. D **46**, 3335 (1992).
[17] A. Babul, T. Piran, and D.N. Spergel, Phys. Lett. B **202**, 307 (1988).
[18] J. Garriga and P. Peter, Class. Quantum Grav. **11**, 1743 (1994).
[19] P. Peter, Class. Quantum Grav. **11**, 131 (1994); P. Peter and D. Puy, Phys. Rev. D **48**, 5546 (1993).
[20] P. Peter, Phys. Rev. D **47**, 3169 (1993).
[21] B. Carter and X. Martin, Ann. Phys. (N.Y.) **227**, 151 (1993); X. Martin, Phys. Rev. D **50**, 7479 (1994).
[22] X. Martin and P. Peter, Phys. Rev. D **51**, 4092 (1995).
[23] B. Carter and P. Peter, Phys. Rev. D **52**, R1744 (1995).
[24] B. Carter and P. Peter, Phys. Lett. B **466**, 41 (1999).
[25] C. Ringeval, Phys. Rev. D **63**, 063508 (2001).
[26] S.C. Davis, W.B. Perkins, and A.C. Davis, Phys. Rev. D **62**, 043503 (2000).
[27] N.K. Nielsen and P. Olesen, Nucl. Phys. **B291**, 829 (1987).
[28] R. Jackiw and P. Rossi, Nucl. Phys. **B190**, 681 (1981).
[29] S.L. Adler and T. Piran, Rev. Mod. Phys. **56**, 1 (1984).
[30] S.A. Fulling, Phys. Rev. D **7**, 2850 (1973).
[31] B.S. Kay, Phys. Rev. D **20**, 3052 (1979).
[32] T. Goto, Prog. Theor. Phys. **46**, 1560 (1971); Y. Nambu, Phys. Rev. D **10**, 4262 (1974).
[33] P. Peter and C. Ringeval, hep-ph/0011308.
[34] C. Ringeval (in preparation).